UNCLASSIFIED

AD NUMBER
AD360624
CLASSIFICATION CHANGES
TO: unclassified
FROM: secret
LIMITATION CHANGES
TO: Approved for public release, distribution unlimited
FROM: Distribution authorized to DoD only; Test and Evaluation; 14 OCT 1960. Other requests shall be referred to Defense Atomic Support Agency, Washington, DC. Formerly Restricted Data.
AUTHORITY
dna ltr dtd 8 Jun 1994; dan ltr dtd 8 jun 1994

THIS PAGE IS UNCLASSIFIED

AD 360624L

WT-1633

This document consists of 60 pages.

No. 209 of 225 copies, Series A

Operation

HARDTACK

April – October 1958

Project 4.1

EFFECTS on EYES from EXPOSURE to VERY-HIGH-ALTITUDE BURSTS (U)

Issuance Date: October 14, 1960

HEADQUARTERS FIELD COMMAND
DEFENSE ATOMIC SUPPORT AGENCY
SANDIA BASE, ALBUQUERQUE, NEW MEXICO

Inquiries relative to this report may be made to

Chief, Defense Atomic Support Agency
Washington 25, D. C.

When no longer required, this document may be destroyed in accordance with applicable security regulations.

DO NOT RETURN THIS DOCUMENT

USAEC Office of Technical Information Extension
Oak Ridge, Tennessee

SECRET

WT-1633

OPERATION HARDTACK—PROJECT 4.1

EFFECTS on EYES from EXPOSURE to VERY-HIGH-ALTITUDE BURSTS (U)

J. E. Pickering, Col, USAF, Project Officer
W. T. Culver, Lt Col, USAF (MC)
R. G. Allen, Maj, USAF
R. E. Benson, Maj, USAF (VC)
F. M. Morris, Maj, USAF (MSC)
D. B. Williams, Maj, USAF
S. G. Wilson, Capt, USAF (MC)
R. W. Zellmer, Capt, USAF (MC)
E. O. Richey

School of Aviation Medicine, USAF
Randolph Air Force Base, Texas

U. S. MILITARY AGENCIES MAY OBTAIN COPIES OF THIS REPORT DI
FROM DDC. OTHER QUALIFIED USERS SHALL REQUEST THROUGH

Director
Defense Atomic Support Agency
Washington, D. C. 20301

FORMERLY RESTRICTED DATA

Handle as Restricted Data in foreign dissemination. Section 144b, Atomic Energy Act of 1954.

This material contains information affecting the national defense of the United States within the meaning of the espionage laws, Title 18, U.S.C., Secs. 793 and 794, the transmission or revelation of which in any manner to an unauthorized person is prohibited by law.

SECRET

FOREWORD

This report presents the final results of one of the projects participating in the military-effect programs of Operation Hardtack. Overall information about this and the other military-effect projects can be obtained from ITR-1660, the "Summary Report of the Commander, Task Unit 3." This technical summary includes: (1) tables listing each detonation with its yield, type, environment, meteorological conditions, etc.; (2) maps showing shot locations; (3) discussions of results by programs; (4) summaries of objectives, procedures, results, etc., for all projects; and (5) a listing of project reports for the military-effect programs.

ABSTRACT

The primary objective was to determine the extent of chorioretinal damage caused by exposure to very-high-altitude, high-yield nuclear detonations at distances of 50 to 350 nautical miles from burst point and to relate experimental data to theoretical calculations. A correlated objective was to estimate, from the data derived from these experiments, distance limits beyond which retinal burns were not expected to occur from nuclear detonations at these altitudes.

Pigmented rabbits were exposed at varying distances from surface zero, on the surface and at altitude, to the radiant thermal energy from two very-high-altitude bursts. Burns were produced in all animals at all stations where line-of-sight vision prevailed.

During Shot Teak (3.8 Mt at about 252,000-foot altitude), chorioretinal burns averaging 0.5 mm in diameter were produced in rabbits exposed behind plexiglass in an aircraft at an altitude of 15,000 feet and a slant range of 307 nautical miles from the burst point.

During Shot Orange (3.8 Mt at about 125,000-foot altitude), similar lesions were produced in rabbits exposed behind plexiglass aircraft windows at an altitude of 24,000 feet and a slant range of 226 nautical miles from the burst point.

It is estimated that comparable burns in the rabbit might well occur on the surface at approximately these same distances when viewed with no intervening attenuator (plexiglass).

From these data it is concluded that all retinal burns occurring within 180 nautical miles would produce a permanent scotoma in the human. Macular involvement especially would reduce visual acuity to a critical level.

PREFACE

The School of Aviation Medicine, USAF, acknowledges the excellent thermal measurements obtained by the Naval Material Laboratory, New York Naval Shipyard, Brooklyn, New York.

Project personnel specifically associated with the thermal project were A. Hirschman, H. Korbel, G. de Lheary, A. Lawes, and J. Mangiola.

During the planning phases of the program, W. Derksen, also from the Naval Material Laboratory, provided invaluable assistance.

CONTENTS

TABLES

FIGURES

Chapter I
INTRODUCTION

1.1 OBJECTIVES

The primary objective was to determine the extent of chorioretinal damage caused by exposure to very-high-altitude, high-yield nuclear detonations at distances of 50 to 350 nautical miles from burst point and to relate experimental data to theoretical calculations. A correlated objective was to estimate, from the data derived from these experiments, distance limits beyond which retinal burns were not expected to occur from nuclear detonations at these altitudes.

1.2 MILITARY SIGNIFICANCE OF CHORIORETINAL BURNS

There is probably more concern in the military for the temporary scotomata of flashblindness than for the permanent chorioretinal burns per se. In the planned methods of saturation nuclear bombing and with the added hazard of antiaircraft missiles equipped with nuclear warheads, the probability of scotomata resulting from viewing an atomic flash could be relatively high. Here, however, the primary concern of the military must be for the physiological effect that might negate the completion of the mission, rather than the resultant pathological change in the retina. To this end, then, applied research is being directed toward development of eye-protective devices to mitigate the physiological hazard (References 1, 2, and 3).

The chorioretinal burn is of minor medical significance when compared to the other hazards of war—particularly a nuclear war. Nevertheless, basic research on the occurrence and severity of chorioretinal burns at varying distances from nuclear detonations is required because of the obvious necessity to deny certain areas to the civilian population during nuclear tests and to establish precautionary procedures for personnel participating in such nuclear tests.

1.3 BACKGROUND

For many years the clinical phenomenon of retinal damage caused by the radiant energy of the sun has been known, and numerous cases have been documented. Most of these cases have occurred while individuals, without eye protection, were watching solar eclipses; thus, this type of retinal lesion has become known as eclipse blindness.

Because the fireball of a nuclear detonation attains internal temperatures comparable to that of the sun, the predicted thermal-energy release is of sufficient magnitude to cause concern about retinal damage in humans who view the detonation without proper eye protection.

During Operation Upshot-Knothole (Reference 1), chorioretinal burns were produced in the eyes of rabbits at distances up to 42.5 miles from ground zero. Also, in four instances, retinal burns were produced accidentally in humans at 2 to 10 miles distance. The burns resulted in permanent scotomata in these individuals. During Operation Redwing (Reference 2), chorioretinal burns were produced in the eyes of rabbits and small primates at distances of 2.7 to 8.1 nautical miles. Some of these burns were produced even though the eye was protected by filters.

The lesions in the above experiments and those produced in eclipse blindness resulted from the same spectral components of electromagnetic radiation—mainly the visible portion with some contribution from the infrared. In general, the difference in degree of retinal damage varies with the rate of energy delivery per unit area. Because eclipse blindness is sustained through a markedly contracted pupil, which limits the amount of radiant energy delivered to the retina, this damage can occur only through protracted exposure. Other factors of importance are, of course, the low rate of delivery of the radiant energy from the sun and the ability of the retina to dissipate the heat by conduction. In the case of a nuclear detonation, however, a large portion of the thermal energy may be delivered to the retina before the protective blink reflex becomes operative. In addition, this exposure may well occur at night when the pupil admits approximately 15 to 25 times the energy that a contracted pupil does in the same time interval, this being only a function of relative pupillary areas. This fact probably accounts for the lack of retinal burns during the Hiroshima incident, because the bomb exploded during bright sunlight when pupils were well contracted.

During Operation Redwing, animals exposed to detonations in the megaton range at sites where the total thermal radiation was of the order of 0.8 to 1.0 cal/cm^2 did not receive chorioretinal burns; on the other hand, animals exposed to detonations of much lower yield, at sites where the total thermal radiation was as low as 0.13 cal/cm^2, did receive burns. This was probably a result of the longer time interval over which the thermal radiation from the higher-yield detonations dissipated itself; much of the total thermal energy reached the exposure site after the rabbit blink reflex (250 to 350 msec) had become operative.

Because, in Operation Hardtack, it was proposed to detonate high-yield weapons at high altitudes, there was grave concern as to the distances at which chorioretinal burns could occur should personnel without eye protection inadvertently view the bursts. Studies were proposed in an effort to establish distance limits beyond which chorioretinal burns would not occur.

1.4 THEORY

The eyeball in the human is nearly an inch in diameter and consists essentially of three separate concentric layers that are modified anteriorly to admit and dominate the passage of light (Figure 1.1). Within these layers a transparent jelly (the vitreous body), a lens, and a fluid (the aqueous humor) are present. The outermost layer, the sclera, is purely protective; the innermost, the retina, is a light-sensitive recorder of images; and the intervening uveal layer consists primarily of the chorioid, which is a nutrient vascular bed for the retina. The chorioid is continued forward as the iris and ciliary body to contain the intraocular muscles that govern the focusing of the lens and pupillary movements.

The cornea is slightly more convex than the rest of the globe so that it forms an anterior prominence. The sclera covers five sixths of the surface of the eye, leaving only two openings, the anterior one that is filled by the cornea and a smaller posterior one for the exit of the optic nerve. The cornea forms the transparent anterior portion of the eyeball and may be likened to the crystal covering a watch face. Behind the cornea lies the anterior chamber which is filled with aqueous humor, which is also optically clear. Behind the anterior chamber lies the lens which, by changing its shape, controls the focus of light rays onto the retina. Between the lens and anterior chamber lies the iris diaphragm which governs the size of the pupillary aperture, thus controlling the amount of incident light. Behind the lens is the vitreous body, which is also optically clear.

The retina is composed of ten layers histologically (the second of which consists of rods and cones) and is a thin light-sensitive membrane, transparent in life (or faintly colored by the visual purple it contains) but an opaque white in death. It lines the whole interior surface of the eye except where it is pierced by the optic nerve head at the optic disc (Figure 1.2). About 3 mm to the temporal side of the disc and slightly below it lies the macula. The fovea centralis is in the center of the macula region. At the fovea centralis, all layers are depleted or absent except the outermost which is composed entirely of cones. It is in this area, the fovea, that visual acuity is maximal and visual acuity decreases on passing peripherally. Thus, at the edge of the macula, visual acuity is reduced about 50 percent; at 7.5 degrees away it is reduced to about 75 percent; and at the extreme periphery to about 3 percent. Actually, acuity is maximal over a plateau 250 microns in diameter at the fovea.

The eye may be compared to a camera. Parallel rays of light are refracted by the cornea, lens, and ocular media so that they are focused on the retina. Should a burn occur directly on the fovea, visual acuity would be markedly decreased. Should it occur in the periphery, there would be less incapacitation, depending on the size of the burn and its location in relation to the fovea. Thus, the optical system of the eye acts as a focusing lens which produces a retinal image of the fireball of a nuclear detonation. Because of this focusing effect, the intensity of thermal radiation on the retina is much greater than the intensity incident upon the eye. Theoretically, neglecting attenuation by air and other media, the radiant energy incident upon the eye will be inversely proportional to the square of the distance from the fireball. However, the

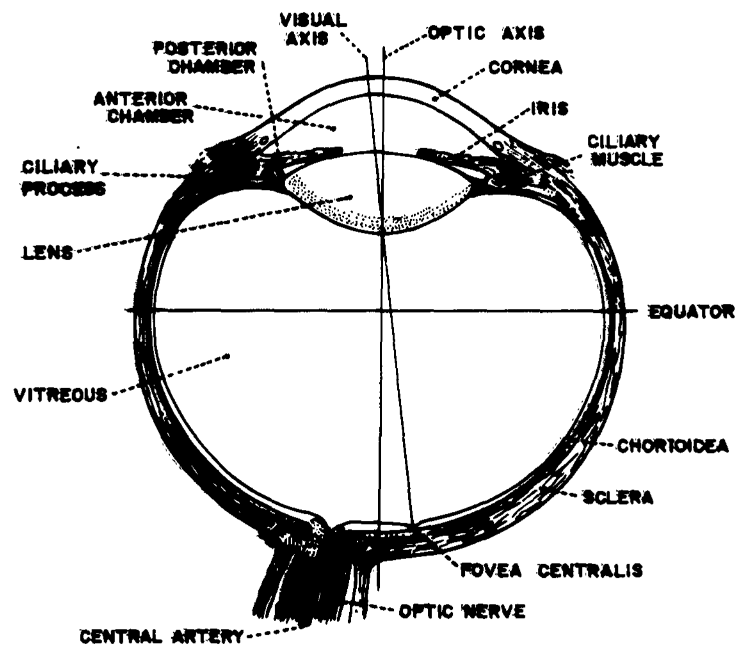

Figure 1.1 Schematic section of right eyeball.

area of the fireball image on the retina is also inversely proportional to the square of the distance from the fireball. The intensity of thermal radiation on the retina is, therefore, independent of the distance from the fireball. The inference, then, is that if a fireball is capable of producing chorioretinal damage, it is capable of producing this damage at great distances. The only difference caused by increasing the distance is that the burn will cover a smaller area. However, the attenuation due to intervening media (air, water vapor, dust, etc.) sharply reduces the distances over which burns will actually occur.

There are other factors that must be considered. The chorioretinal damage produced is dependent on the rate of delivery of the radiant energy on the area of the fireball image, and on the total energy delivered. If the radiant exposure at the retina is below the rate at which the energy can be dissipated by the retina, there will be no damage. The total time of exposure must also be considered. The normal blink reflex of about 300 msec in rabbits and 50 to 150 msec in man will limit exposure to that period of time. Only that radiation received before the blink reflex becomes operative, rather than the total thermal radiation, is of importance in causing chorioretinal damage. Data derived from Shot Yucca during Operation Hardtack (Reference 4) clearly suggests that the total thermal energy for a high-altitude burst will be delivered in the order of 20 to 35 msec, which period is well before the blink reflex time.

A further consideration is the pupillary radius, because the energy delivered to the retina is directly proportional to the square of the radius of the pupil. Because the pupil is larger during darkness, the possibility exists that threshold distances might well be greater at night than during daylight hours for shots of comparable characteristics. In addition, the attenuation of the radiant energy by the intraocular media must be considered. Because there was no available data on the transmission characteristics of these media, an arbitrary fractional-transmission coefficient was selected, on the basis of transmission coefficients of similar tissue.

Other factors are introduced by a high-altitude burst. The reduced attenuation, higher thermal output, and a shorter thermal-energy delivery time can result in chorioretinal damage at distances and for yields that would present no problem for surface or low-altitude bursts.

1.4.1 Incidence Angle of Radiation at Observation Point. Of considerable importance is the angle of incidence of the thermal radiation on the observation point. Very small angles of in-

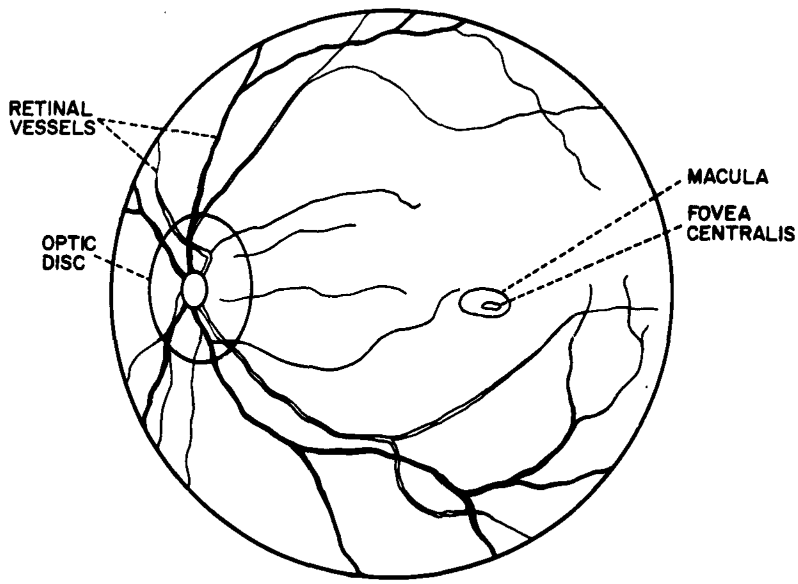

Figure 1.2 Drawing of posterior, inner aspect of the eye.

cidence imply that the radiation proceeds for a considerable distance through the dense lower atmosphere and thus is attenuated more rapidly. In addition, the curvature of the earth precludes viewing the fireball at some given distance, depending upon the height of the burst and the height of the observation point. For this experiment, calculations of various angles of incidence were necessary to position the experimental animals as accurately as possible so that a high probability of viewing the fireball would be attained.

Figure 1.3 is a plot of the angle of incidence as it varies with the distance, on the ground, from ground zero, for detonations at 252,000 feet (Shot Teak) and 125,000 feet (Shot Orange). In addition, the angles of incidence from these shots as might be experienced by aircraft at various altitudes and at varying distances are shown in Figures 1.4 and 1.5. The expressions from which these data were obtained are given below.

Surface observation point:

$$\gamma = \cos^{-1}\left\{\frac{S\,[1 + H/(2R) - S^2/(8R^2)]}{(S^2 + H^2)^{1/2}}\right\}$$

Where: γ = angle of burst above horizon in degrees
H = altitude of burst in nautical miles
R = radius of earth (3,437.8 nautical miles)

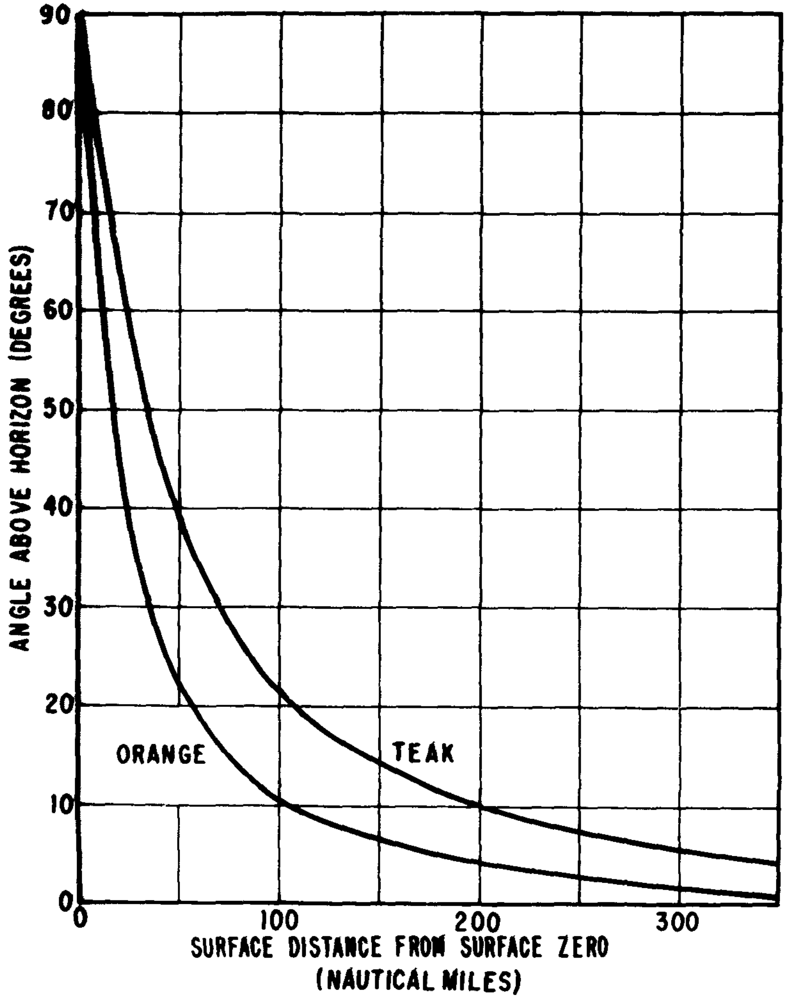

Figure 1.3 Angle of burst above horizon versus surface distance.

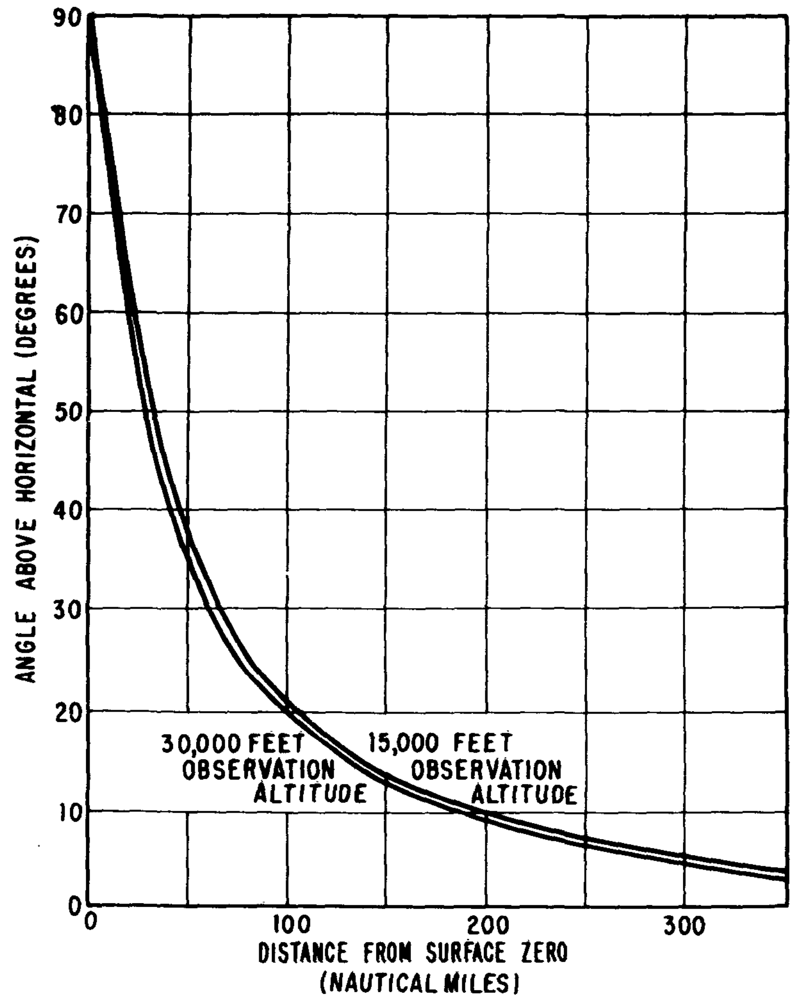

Figure 1.4 Angle of burst above horizontal versus surface distance, Shot Teak.

S = surface distance from ground zero, nautical miles (see Figure 1.6)

Altitude observation point:

$$\gamma_A = \cos^{-1}\left\{\frac{S(1 + A/R)\left[1 + \frac{H - A}{2(R + H)} - \frac{S^2(1 + A/R)^2}{8(R + A)^2}\right]}{\left[(H - A)^2 + S^2(1 + A/R)^2\right]^{1/2}}\right\}$$

Where: γ_A = angle of burst above horizontal in degrees
A = altitude of observation, nautical miles

1.4.2 Threshold of Energy Required to Produce Retinal Burns. At the rates of radiant energy under consideration (greater than 5 cal/cm^2 delivered to the retina in 0.2 second or less), it has been estimated (References 4, 5, and 6) that there is a threshold of energy incident on the retina required to produce retinal burns and that this threshold varies with the size of the fireball image on the retina. Figure 1.7 (Reference 5) shows the variation of estimated threshold energy with image size. The curve implies that the minimum image diameter that will sustain a burn is about 0.1 mm.

1.4.3 Diameter of Fireball Image on the Retina. The diameter of the fireball image should follow the simple law of geometrical optics:

$$d_r = \frac{F}{D} d_{fb}$$

Where: d_r = diameter of image on retina, mm
F = focal length of eye
D = distance from fireball to image, cm
d_{fb} = diameter of fireball, mm

The diameter of the fireball image on the retina was calculated using the assumptions that (1) the effective fireball diameter would be 7 km for Shot Teak and 4 km for Shot Orange (References 4 and 7), (2) the distance was taken from the center of the fireball to the retina, and (3) the average focal length in the rabbit eye is 1.5 cm. Figure 1.8 indicates the variation of image diameter with distance along the surface from surface zero. Figures 1.9 and 1.10 are equivalent graphs of image size at various distances and altitudes in the ranges in which the airborne exposure stations were positioned.

1.4.4 Unscattered Irradiance Dose at Observation Point. To reasonably position experimental animals, it was desirable to estimate the irradiance as a function of distance from burst point (or from surface zero). Because of uncertainties in the anticipated thermal spectrum and in the atmospheric composition, and the unavailability of appropriate air absorption and scattering coefficients, an effort was made to estimate the unscattered irradiance as a function of distance from surface zero for a range of assumed attenuation coefficients. The attenuation coefficients were selected to correspond to narrow-beam transmissions at sea level for standard, clear, dry air of 98, 95, 93, and 90 percent transmission per nautical mile. These assumptions gave the following coefficients:

$k_1 = 8.346 \times 10^{-5}$ cm^2/gm (98 pct/nm)

$k_2 = 2.128 \times 10^{-4}$ cm^2/gm (95 pct/nm)

$k_3 = 3.088 \times 10^{-4}$ cm^2/gm (93 pct/nm)

$k_4 = 4.382 \times 10^{-4}$ cm^2/gm (90 pct/nm)

The transmission through an atmosphere of varying density and composition may be calculated

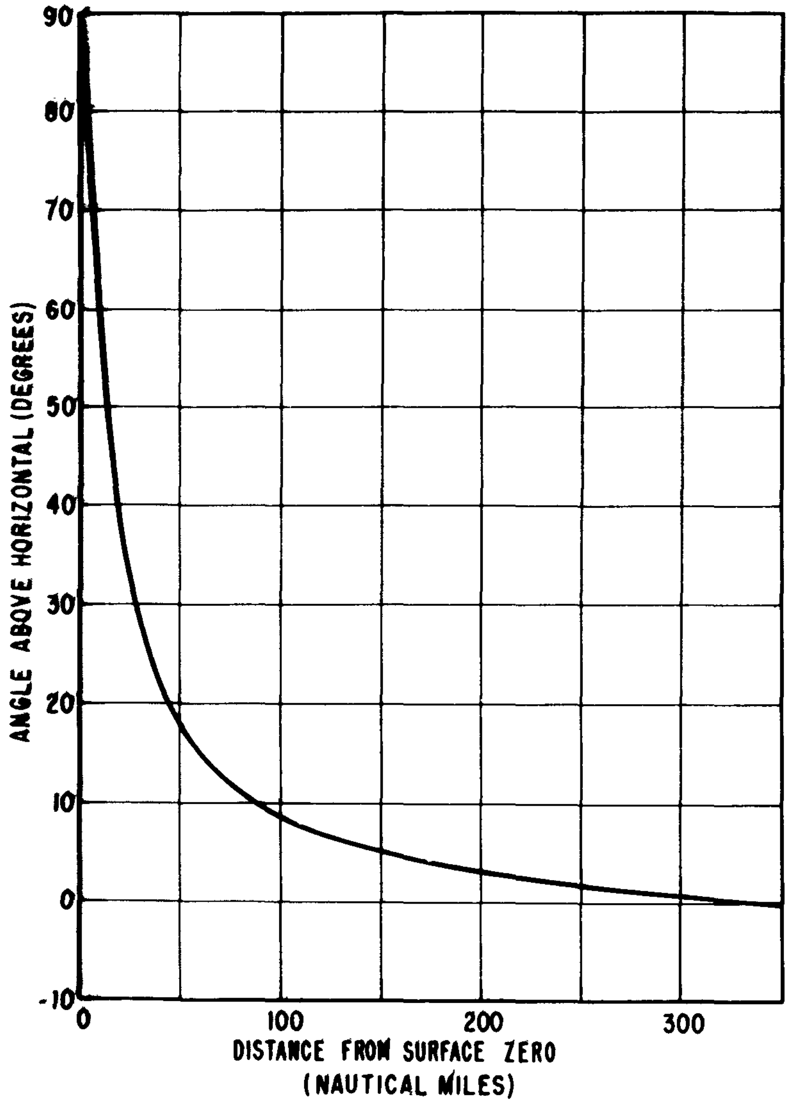

Figure 1.5 Angle of burst above horizontal versus surface distance, Shot Orange (observation altitude 25,000 feet).

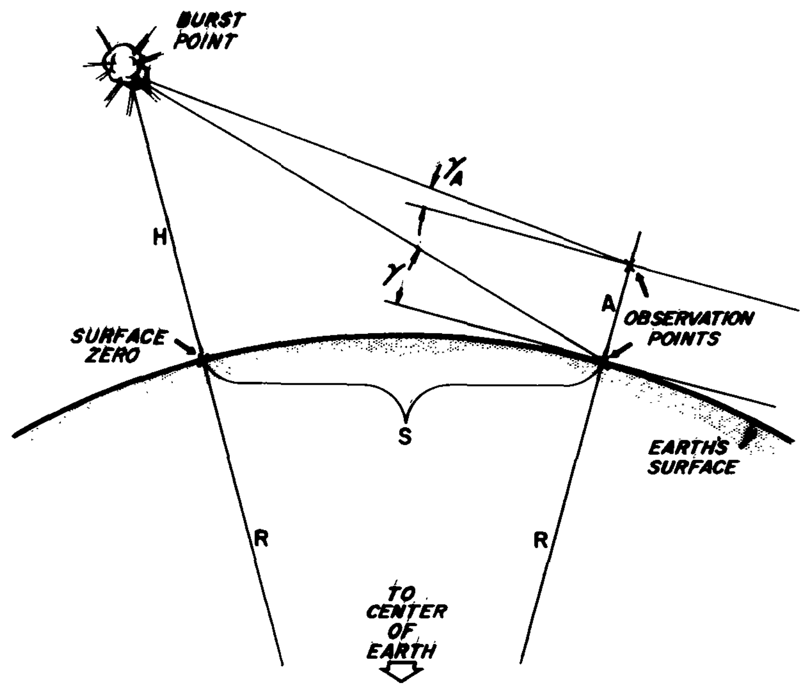

Figure 1.6 Geometric diagram illustrating parameters used in calculation of angles of incidence at various observation points.

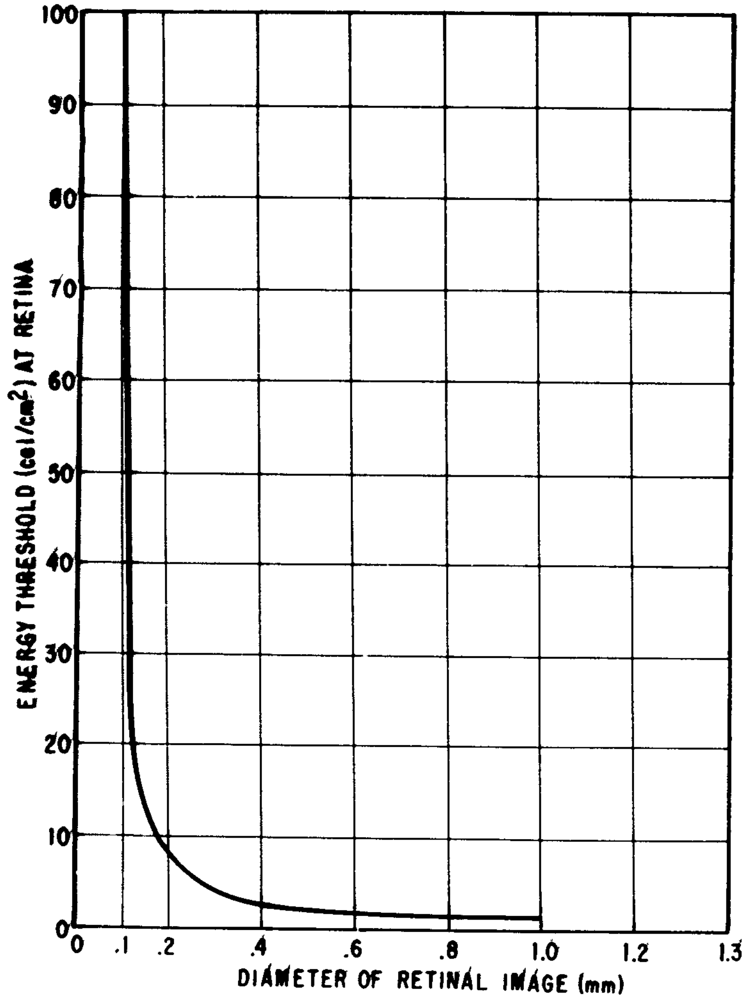

Figure 1.7 Threshold radiant exposure for retinal burns versus retinal image diameter.

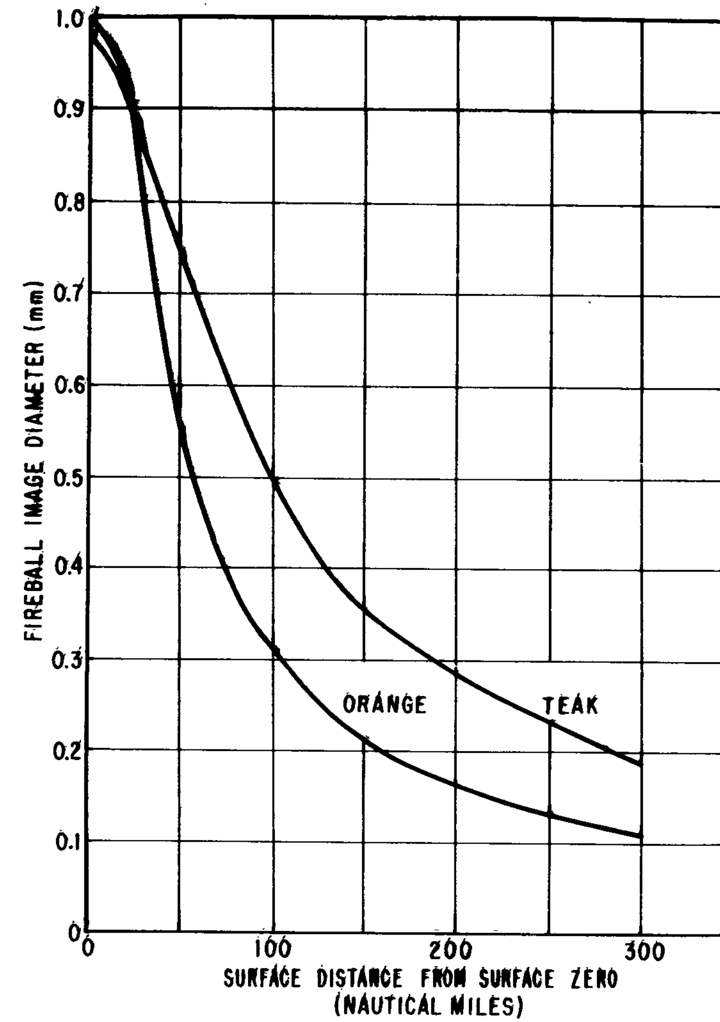

Figure 1.8 Fireball image diameter for surface exposure sites versus surface distance. Shot Teak: assumed effective fireball diameter, 7 km. Shot Orange: assumed effective fireball diameter, 4 km.

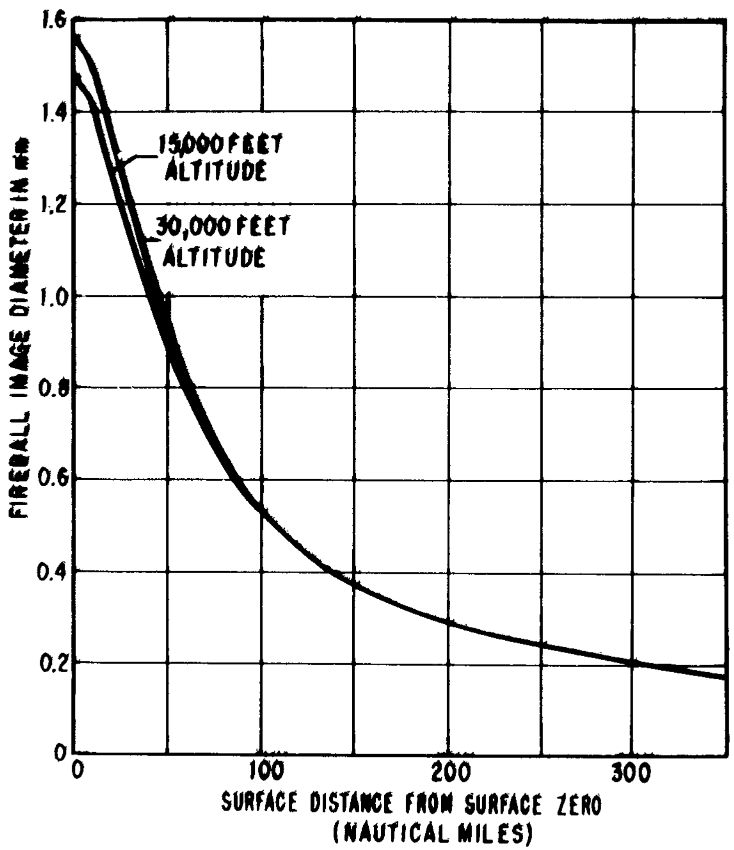

Figure 1.9 Fireball image diameter for airborne exposure sites versus surface distance, Shot Teak. Assumed effective fireball diameter, 7 km.

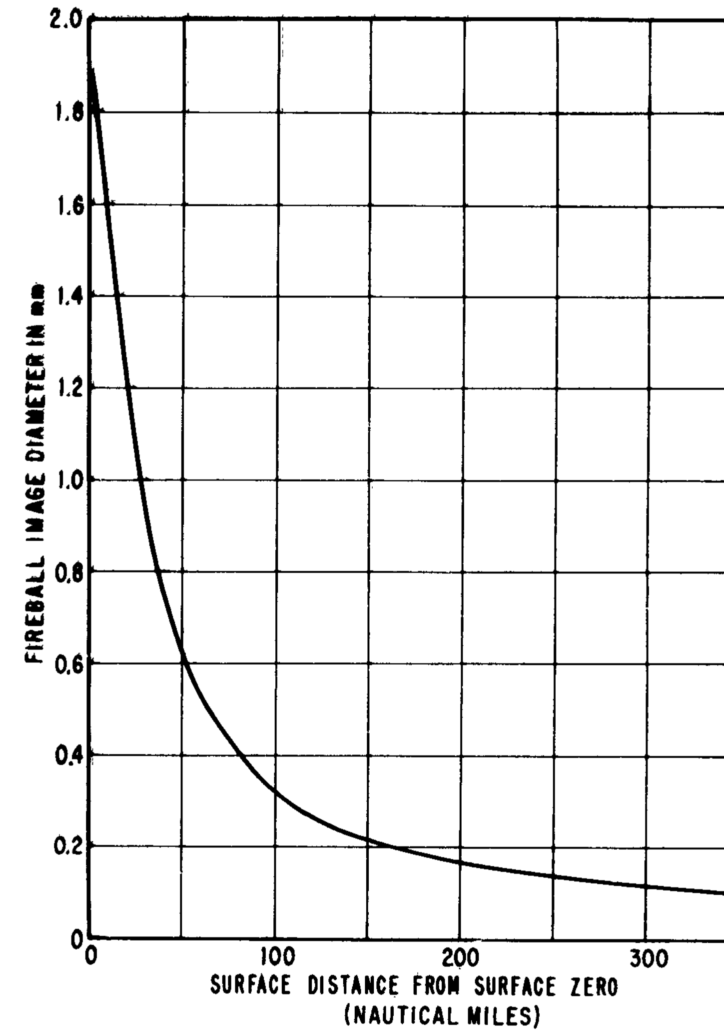

Figure 1.10 Fireball image diameter for airborne exposure sites versus surface distance, Shot Orange. Observation altitude, 25,000 feet; assumed effective fireball diameter, 4 km.

by assuming an average attenuation coefficient, as above, or perhaps more realistically, by assuming different attenuation coefficients for various portions of the path length. For this approximation an attenuation coefficient of 3.088×10^{-4} was used up to an altitude of 1 nautical mile. A value of 2.128×10^{-4} was used for that portion of the path falling between a 1- and 2-nautical mile altitude, and 8.346×10^{-5} was used as the attenuation coefficient above 2 nautical miles.

The variation in air density with altitude was assumed to be exponential and to obey the relation

$$d = d_0 e^{-qH}$$

Where: H = altitude in nautical miles
d = air density, gm/cm^3
q = 0.2324 (nautical miles)$^{-1}$
d_0 = sea-level air density, gm/cm^3

The curvature of the earth was taken into consideration in the calculations.

On the basis of these assumptions, the unscattered radiant exposure at the eye, Q_p, in calories per square centimeter is given by:

$$Q_p = \frac{a f p W_{kt} \times 10^{12}}{4 \pi D^2} e^{-k I_1}$$

Where: $$I_1 = 18.492 \times 10^4 d_0 \int_0^{(H^2 + S^2)^{1/2}} e^{q \left\{ R - \left[x^2 + \frac{2HR - S^2)x}{(H^2 + S^2)^{1/2}} + R^2 \right]^{1/2} \right\}} dx$$

Correspondingly, the unscattered radiant exposure on the retina, Q_r, in calories per square centimeter is given by:

$$Q_r = T_E (r_p/F)^2 (D/r_{fb})^2 Q_p$$

Where: a = spectral-attenuation factor (a = 0.5)
f = fraction of total thermal energy emitted during blink reflex
p = fractional thermal partition
W_{kt} = total yield, kilotons
H = altitude of burst, nautical miles
S = surface distance from ground zero, nautical miles
d_0 = sea-level air density, gm/cm^3
k = air-attenuation coefficient, cm^2/gm
q = coefficient of air density variation with altitude
R = earth's radius, nautical miles
r_{fb} = radius of fireball, cm
F = focal length of eye, cm
T_E = fractional transmission of eye system
r_p = radius of pupil, cm
D = slant distance from burst to point of observation, cm

The results of the calculations using $p = \frac{1}{2}$, $f = 1$, and W_{kt} = 4 Mt are given for Shots Teak and Orange in Figures 1.11 through 1.14.

Using data from Figures 1.11 through 1.14 and 1.7 through 1.10, estimates of the maximum distances for which chorioretinal burns were anticipated were obtained.

Estimates of the unscattered radiant exposure at altitude were made neglecting the curvature of the earth. The expressions used for these calculations were:

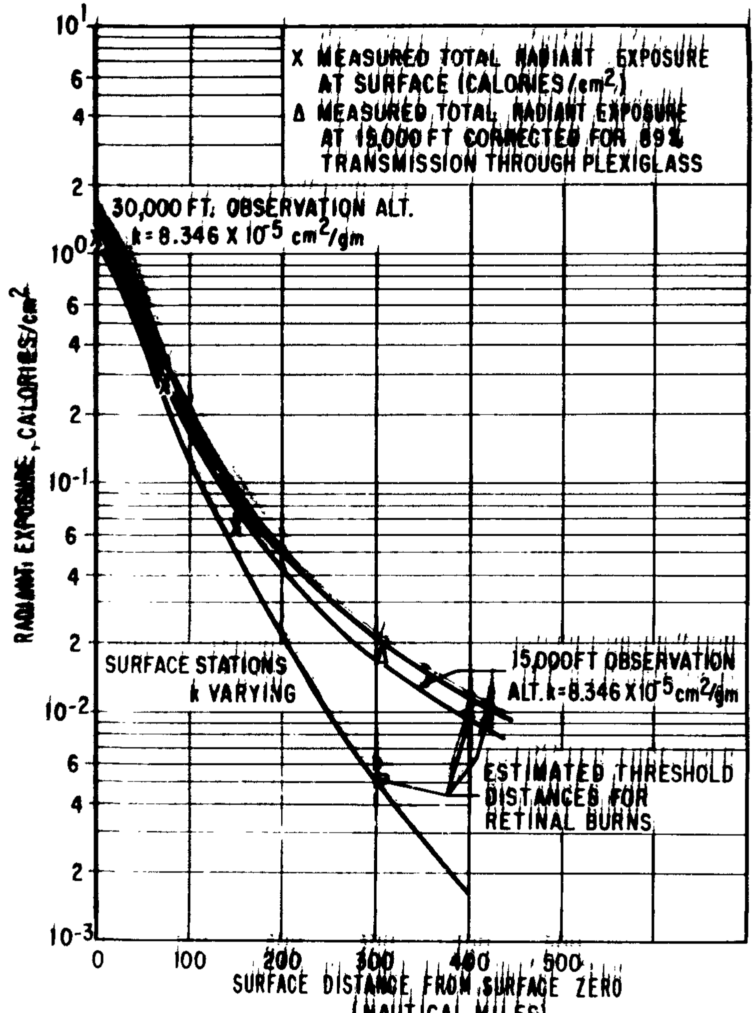

Figure 1.11 Calculated unscattered radiant exposure at exposure sites versus surface distance, Shot Teak.

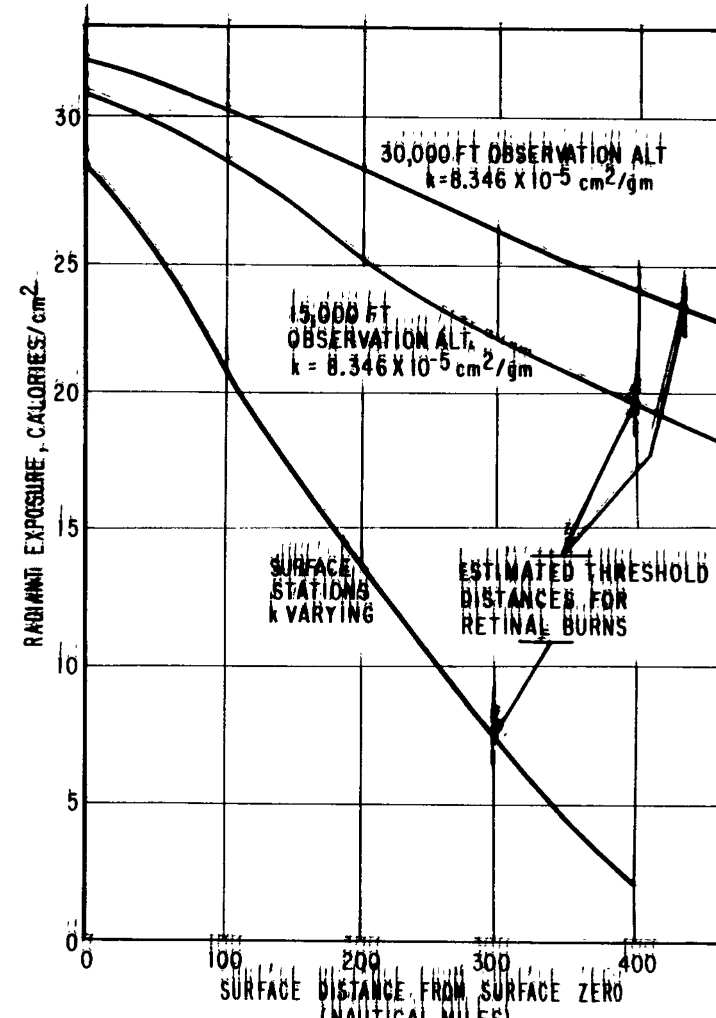

Figure 1.12 Calculated radiant exposure at retina versus surface distance, Shot Teak. Assumed effective fireball diameter, 7 km.

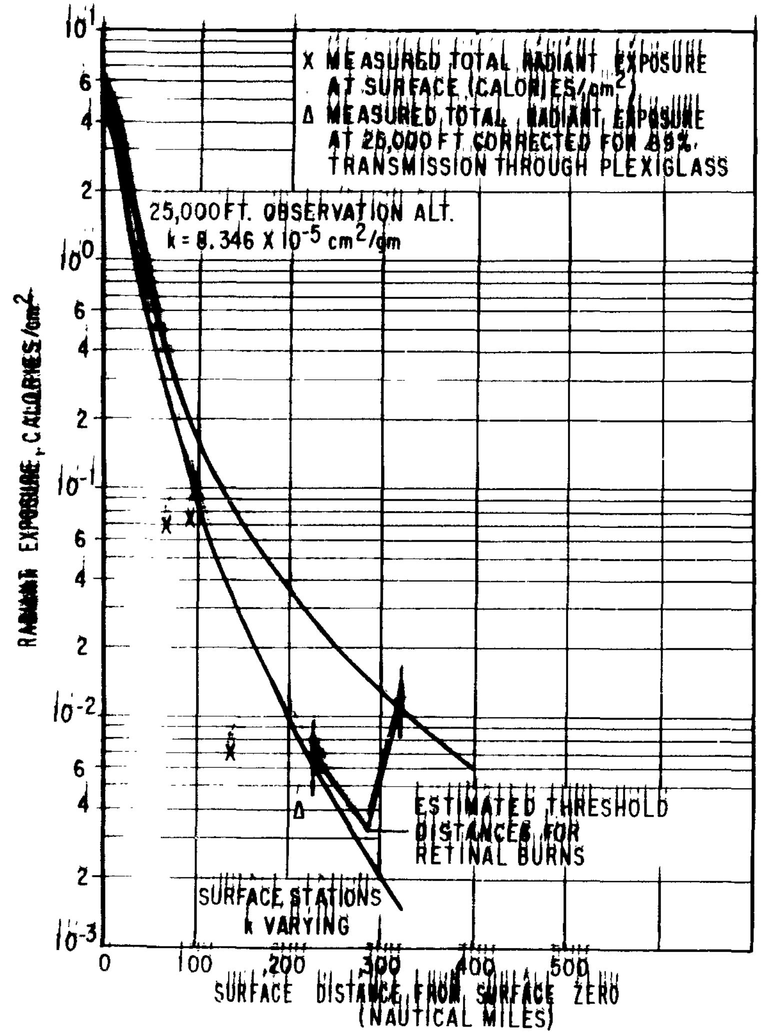

Figure 1.13 Estimated unscattered radiant exposure at exposure sites versus surface distance, Shot Orange.

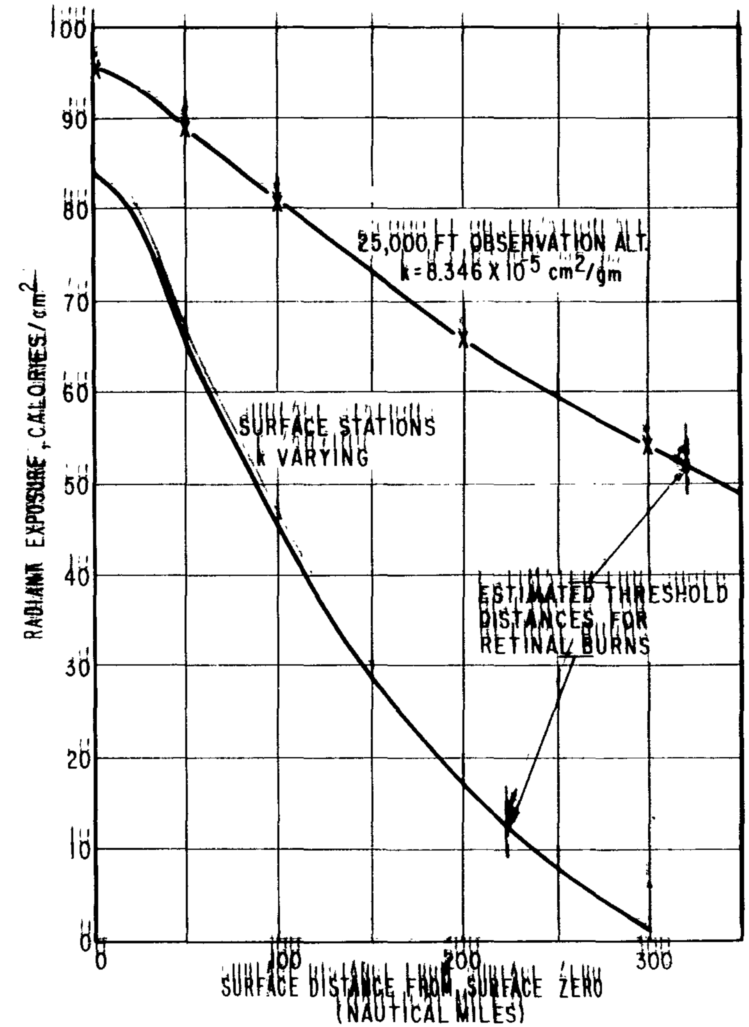

Figure 1.14 Calculated radiant exposure at retina versus surface distance, Shot Orange. Assumed effective fireball diameter, 4 km.

$$Q_{pA} = \frac{a f p W_{kt} \times 10^{12}}{4 \pi D^2} e^{-k I_2}$$

Where: $$I_2 = \frac{1,030 \left[(H - A)^2 + S^2\right]^{1/2}}{(H - A)} e^{-qA} \left[1 - e^{-q(H - A)}\right]$$

And: $$Q_{rA} = T_E (r_p/F)^2 (D/r_{fb})^2 Q_{pA}$$

Where: H = altitude of burst, nautical miles

A = altitude of observation station, nautical miles

It is recognized that these calculations depend upon the assumption of numerical values for several parameters for which no adequate data were available, e.g., an average fireball diameter, over the time of exposure, which produces an image with sufficient intensity to cause retinal damage (effective fireball diameter).

Spectral effects were not treated specifically. These effects were considered only indirectly by normalizing the calculated, unscattered radiant exposure with the measured exposure at the Johnston Island station for Shot Teak (spectral attenuation factor, a = 0.55). No such normalization factor was available for Shot Orange because of cloud cover. Consequently, this same factor was used for Shot Orange.

Finally, the atmospheric attenuation was admittedly a crude approximation. However, it is questionable whether a more sophisticated approach would yield results which could be readily reduced to rules of general applicability.

Chapter 2
PROCEDURE

2.1 SHOT PLANNING

The concern of responsible personnel over the possibility of retinal burns in native populations living at some distance from the Eniwetok Atoll dictated that the high-yield, high-altitude shots during Operation Hardtack be removed to Johnston Island.

It was obvious that, to establish distance limits beyond which retinal burns could be expected not to occur, exposure stations on the earth's surface should extend to at least 150 nautical miles, and preferably to 300 miles from Johnston Island. This was certainly true for Shot Teak. Furthermore, because of the normal cloud distribution over the ocean during July and August, the probability of an unobstructed line of sight was quite small. For this reason and because collection of positive data was important, a near station at or near the theoretical limit for producing retinal burns was also necessary. Within these limitations, reasonable data were to be expected from the positioning of rabbits and thermal-recording devices at the exposure stations listed below.

For Shot Teak, the stations were at (1) Johnston Island; (2) the USS DeHaven, a destroyer, approximately 70 nautical miles from Johnston; (3) the USS Cogswell, a destroyer, approximately 150 nautical miles from Johnston; (4) the USS Hitchiti, a seagoing tug, approximately 305 nautical miles from Johnston; (5) and (6) two B-36s of Program 9 flying at 30,000 feet at a distance of 44 nautical miles; and (7) a C-97 aircraft flying at an altitude of 15,000 feet at approximately 305 nautical miles from surface zero.

For Shot Orange, the stations were on (1) the USS Boxer, a carrier, 50 nautical miles from Johnston Island; (2) the USS Epperson, a destroyer, at 65 nautical miles; (3) the USS DeHaven at 190 nautical miles; and (4) a C-97 aircraft at 205 nautical miles and an altitude of 24,000 feet.

Table 2.1 indicates the station locations and the estimated radiant exposure on the retina at these stations.

2.2 OPERATIONAL PROCEDURES

Project 4.1 was based on Johnston Island and on Oahu, T.H. Rabbit examination and data evaluation were performed at both places. Exposure stations on Johnston Island, the USS Boxer, and the destroyers were supported and maintained from Johnston Island. Three project personnel were located at Hickam Air Force Base, Oahu, to prepare and maintain the airborne exposure stations and the one on the tug.

On D-2 days, Shot Teak, the seagoing tug departed Pearl Harbor for the 305-nautical-mile station. Two project personnel and the necessary rabbits were aboard. At H-3 hours, the rabbits were removed from their transport cages and placed in the exposure boxes, which were then positioned in the exposure racks. The rabbits were under continuous surveillance, and at H-15 seconds from voice countdown, it was assured that all were alert. As soon as possible after exposure, they were placed back in their transport cages. The tug returned to Pearl Harbor, and the rabbits were then transferred to Hickam AFB.

At H-12 hours, the two destroyers departed Johnston Island and proceeded to their stations. Two project personnel were aboard each of them, along with the necessary rabbits and supplies. As soon as possible after exposure, the rabbits were replaced back in their transport cages and returned to Johnston Island.

At H-8 hours, the exposure station on Johnston Island was readied by project personnel.

were evacuated to the USS Boxer. As soon as possible after the exposure of the rabbits, the personnel returned to the island, removed them to their living cages, and proceeded to evaluate retinal damage.

At H–5 hours, rabbits were placed in exposure racks in the aircraft (RB-36's and C-97) at Hickam AFB, and the aircraft proceeded to their positions. No project personnel were aboard the RB-36's, but the rabbits were awakened at H–15 seconds by the built-in alarm-bell system. The rabbits in the C-97 were accompanied by one person who was responsible for seeing that they were awake at the proper time. As soon as the aircraft returned, the rabbits were transferred to living cages to await retinal evaluation.

For Shot Orange, the procedure was similar except for the obvious changes in positions and number of the exposure stations.

2.3.3 INSTRUMENTATION

2.3.3.1 Holding Boxes and Exposure Racks. Specially designed holding boxes for the rabbits (Figures 2.1 and 2.2) were used so that the head would be immobilized for exposure and subse-

TABLE 2.1 SUMMARY OF STATIONS, LOCATIONS, AND ESTIMATED RADIANT EXPOSURES FOR SHOTS TEAK AND ORANGE

Station Location for Shots: Teak	Orange	Horizontal Distance from Surface Zero	Slant Range from Burst Point	Elevation	Azimuth	Altitude	Estimated Radiant Exposure at Station	Estimated Radiant Exposure at [illegible]	Number of Rabbits
		naut mi	naut mi	deg	deg	ft	cal/cm²	cal/cm²	
Johnston Island	—	[illegible]	41	83	0	Surface	[illegible]	28	5
—	USS Boxer	70	73	15	030	Surface	0.25	56	8
USS [illegible]	—	77	79	28	030	Surface	0.23	22	11
—	USS [illegible]	85	88	11	030	Surface	0.13	50	8
—	USS [illegible]	144	144	7	030	Surface	0.085	31	8
USS [illegible]	—	136	135	13	030	Surface	0.05	17	12
USS [illegible]	—	305	307	5	006	Surface	[illegible]	7	12
RB-36 No. 1	—	64	71.6	22	006	38,000	0.35	31	4
RB-36 No. 2	—	64	71.6	22	006	38,000	0.35	31	4
C-97	—	305	307	5	006	15,000	[illegible] *	13 *	8
—	C-97	225	226	2	006	20,000	[illegible] *	48 *	8

* Assumes 50 percent transmission [illegible] aircraft windows.

quent examination and photography. For the ground and ship exposure stations, wooden A-frames with racks (Figures 2.3, 2.4, and 2.5) were constructed. The frames could be positioned either upright or horizontally to correct for differing angles of incidence. Figure 2.6 shows the racks in position on Johnston Island, and Figure 2.7 shows them in position on a destroyer.

Racks for four rabbits were designed to fit the radio compartment blisters of the RB-36's (Figures 2.8 and 2.9). Racks for two rabbits were designed for placement at the windows in the C-97 aircraft (Figure 2.10).

2.3.3.2 Supporting Photography and Timing Signals. These aspects of instrumentation were handled by Task Force personnel. Cameras were in position to photograph the rabbits' eyes and, simultaneously, to photograph the cloud cover during exposure. This gave information as to whether the animals' eyes were open and whether there were intervening clouds at exposure time. Except for the C-97, no cloud photography was done at the airborne exposure stations; the RB-36's were [illegible] above the cloud cover.

Timing signals were voice countdown in all cases and were transmitted by radio to all stations except Johnston Island. On Johnston, the [illegible] cameras were set and triggered to run from H–5 seconds to H+25 seconds. The [illegible] cameras at the shipboard and airborne stations were triggered manually.

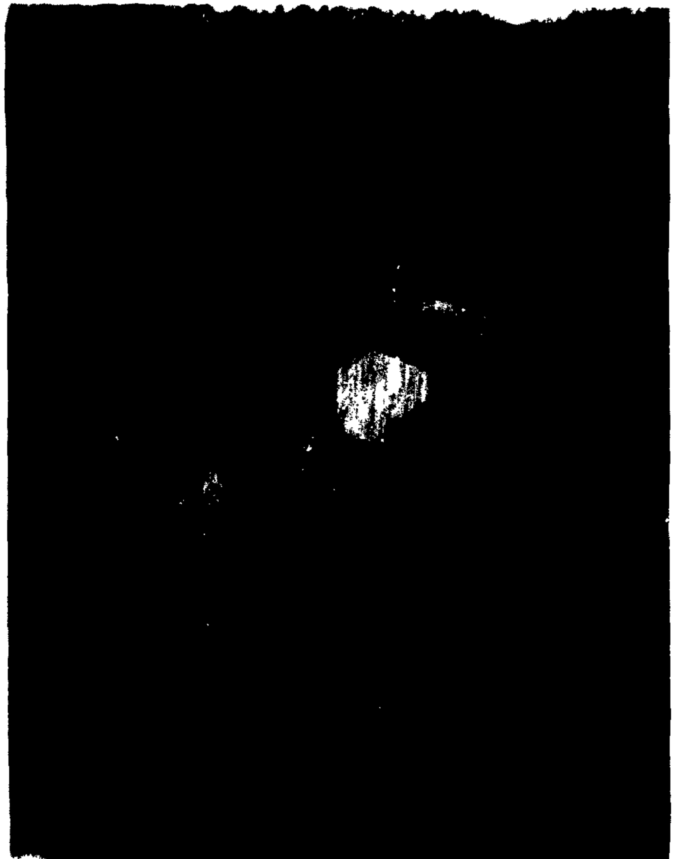

Figure [illegible] Rabbit-holding box designed for exposure and examination.

Figure [illegible] Rabbit in place in holding box.

SECRET

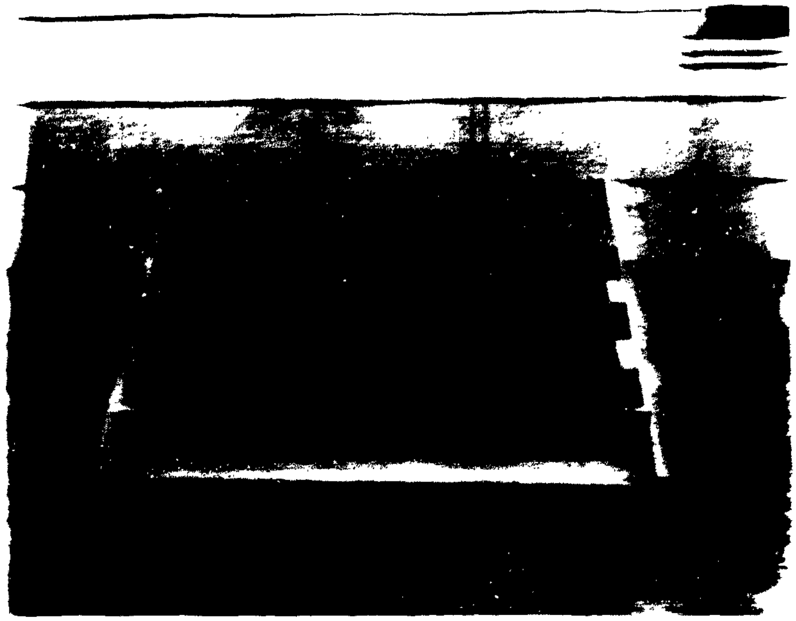

Figure [illegible] 2.3 [illegible] for high angle of incidence.

Figure [illegible] 2.4 [illegible] for high angle of incidence.

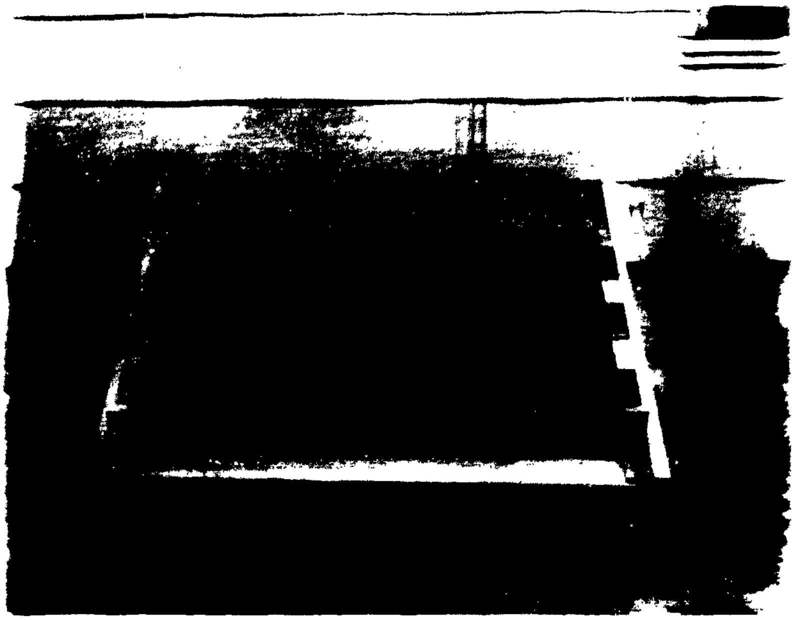

Figure 23 [illegible] position for high angle of incidence.

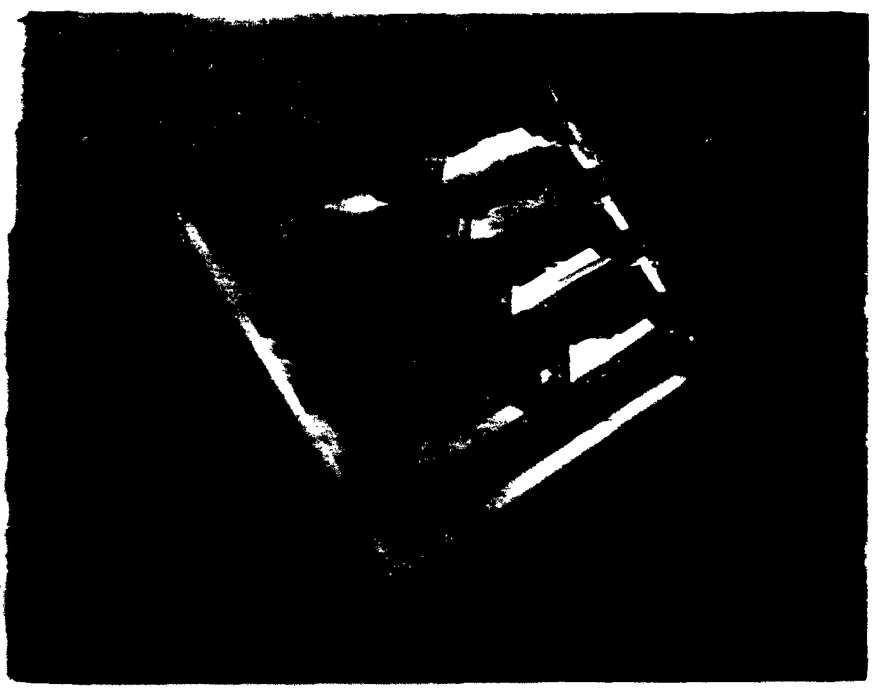

Figure 24 [illegible] used for high angle of incidence.

Figure 25 Pallets and holding boxes in A-frame in upright position.

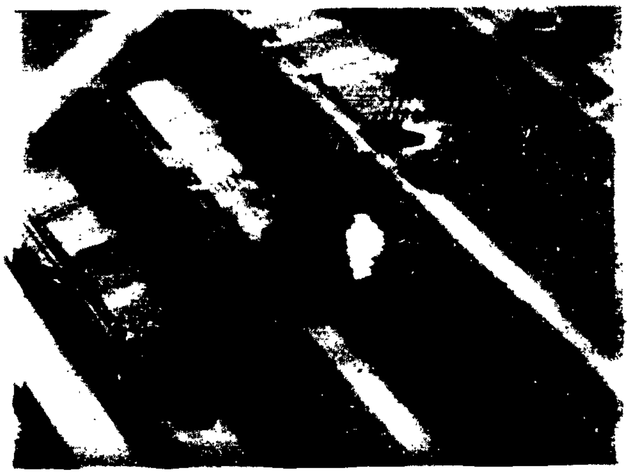

Figure 26 Pallets in overpressure racks, J[illegible] and [illegible].

Figure 27 Pallets in overpressure racks, and thermal measuring equipment and cables.

Figure 28 Exposure racks and holding boxes in B-36 blister, rear view.

Figure 29 [illegible] in position in B-36 blister, front view.

2.3.3 Thermal-Energy Measurements. Data for thermal evaluation were obtained from measurements by Projects 8.2, 8.3, and 8.4 at the exposure stations on the B-36's. Thermal measurements at all other exposure stations were made by Project 8.1. Because of the inadequacy of preparation time, it was impossible to instrument properly to gain complete spectral measurements of the thermal energy from Shots Teak and Orange.

2.4 ANIMAL CARE AND EVALUATION

Sixty-four pigmented rabbits of both sexes, weighing between $4\frac{1}{2}$ and $7\frac{1}{2}$ pounds, were se-

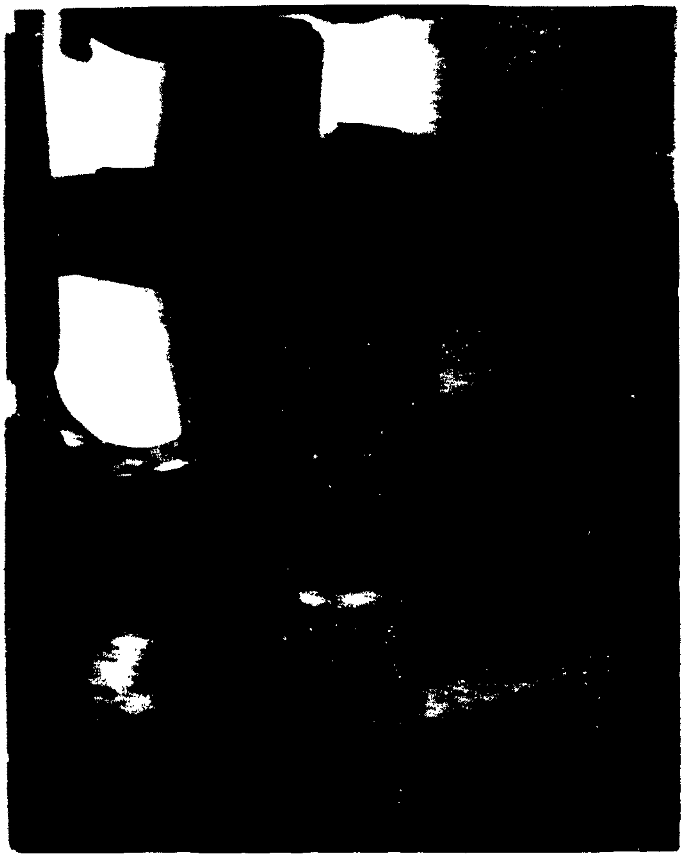

Figure 2.10 Exposure rack holding boxes in C-97.

lected for the study. The rabbits were procured from various sources throughout the United States and were housed at Randolph AFB for 3 weeks prior to shipment to Johnston Island. During this period they were treated with Canex to eliminate ear mites, Sulmagyl to decrease the incidence of diarrhea that are prevalent in this experimental animal, and Combiotic for general, broad-spectrum prophylaxis.

Each rabbit was numbered by tattoo, and the right ear was marked for ease of rapid identification. Each rabbit was baselined with ophthalmoscopy and retinal photographs obtained with the Zeiss-Contax retinal camera. Figure 2.11 shows ophthalmoscopic examination of a rabbit and the use of the holding box for this purpose. Figure 2.12 illustrates the use of the retinal camera with a rabbit as a subject.

At Johnston Island and Hickam AFB, the rabbits exposed during Shot Teak were given an ophthalmoscopic examination, their retinas were photographed, and the damage was evaluated.

Figure 2.11 Ophthalmoscopic examination of rabbit.

Figure 2.12 Retinal photography of rabbit.

Atropine sulfate, ½-percent solution, was used for pupillary dilatation. Sedation, when necessary, was accomplished with sodium pentathol, or thorazine.

After Shot Orange, these procedures were re-accomplished on the contralateral eye.

Selected rabbits were sacrificed and their eyes enucleated and preserved for further gross and microscopic pathologic study at the School of Aviation Medicine (SAM), USAF; others were returned to SAM for long-term follow-up.

Chapter 3
RESULTS

The detailed results are shown in the tables of this section. The pathology of the retinal burns and the photographic evidence, both gross and microscopic, are discussed in Chapter 4.

3.1 SHOT TEAK

3.1.1 Thermal Measurements. A summary of the data of Project 8.1 is shown in Table 3.1. A detailed discussion of these data is contained in the Appendix. It was technically impossible to measure the radiant dose at the retina at this time, but the experimental results indicate that

TABLE 3.1 SUMMARY OF THERMAL MEASUREMENTS, CLOUD COVER, AND RETINAL LESIONS, SHOT TEAK

Station	Slant Range from Burst Point	Radiant Exposure (Black Body Receiver) at Station	Retinal Lesion Diameter (Average Lesion)	Type of Cloud Cover	Line of Sight to Detonation
	naut mi	cal/cm^2	mm		
Johnston Island	41	1.2	2.2	Clear	Unobstructed
USS DeHaven	79	0.27	1.6	Strato cumulus	Unobstructed
USS Cogswell	155	0.066	0.99	Strato cumulus	Unobstructed
USS Hitchiti	307	0.0007*	0.00	Strato cumulus	Obstructed
B-36 No. 1	73.8	—	1.8	Clear	Unobstructed
B-36 No. 2	73.8	—	1.8	Clear	Unobstructed
C-97	307	0.015†	0.5	Clear	Unobstructed

* Scattered thermal radiation.
† Measured through plexiglass aircraft window.

the assumptions made for transmission of energy through the media of the eye were reasonable. Table 3.1 also indicates the type of cloud cover at shot time for the various exposure stations and whether the line of sight from the rabbits to the detonation point was obstructed, as well as the diameter of representative lesions at each station.

3.1.2 Blink-Reflex Time. No attempt was made to measure the time required for the rabbits to blink after the stimulus of the light flash. Blink-reflex time has been measured previously, and it was assumed that the total thermal energy from the detonation would be delivered well within the blink-reflex time. Thus, it was only necessary to know that the rabbits' eyes were open during the time of the thermal flash. Figure 3.1 is a representative photograph of the rabbit eyes taken at the time of the detonation. Table 3.2 denotes the condition of the rabbits' eyes at time of detonation, the percent of retinal burns, and average size of the burns.

3.2 SHOT ORANGE

The thermal measurements of Project 8.1 during Shot Orange are shown in Table 3.3. Because of more atmospheric attenuation, the exposure station distances were changed for this

Figure 3.1 Condition of rabbits' eyes (open or closed) at time of detonation at 300-mile surface station, Shot Teak.

TABLE 3.2 CONDITION OF RABBITS' EYES AT EXPOSURE TIME, PERCENT RETINAL BURNS, AND AVERAGE BURN SIZE, SHOT TEAK

Station	Number of Rabbits	Condition of Eye	Retinal Burns	Average Lesion Diameter
			pct	mm
Johnston Island	5	Open	100	2.2
USS DeHaven	11	Open	100	1.6
USS Cogswell	12	Open	100	0.99
USS Hitchiti	12	Open	0	—
B-36 No. 1	4	Open	100	1.6
B-36 No. 2	4	Open	100	1.8
C-97	8	Open	100	0.5

TABLE 3.3 SUMMARY OF THERMAL MEASUREMENTS, CLOUD COVER, AND RETINAL LESIONS, SHOT ORANGE

Station	Slant Range from Burst Point	Radiant Exposure (Black Body Receiver) at Station	Retinal Lesion Diameter	Type of Cloud Cover	Line of Sight to Detonation
	naut mi	cal/cm^2	mm		
USS Boxer	73	0.07 *	0	Strato cumulus	Obstructed
USS Epperson	88	0.075	0.8	Strato cumulus	Unobstructed
USS DeHaven	141	0.007 *	0	Strato cumulus	Obstructed
C-97	226	0.0035	0.4	Clear	Unobstructed

* Scattered radiation cloud cover.

Figure 3.2 Cloud cover in line of sight from 141-mile surface station (USS DeHaven) to detonation point, Shot Orange.

TABLE 3.4 CONDITION OF RABBITS' EYES AT EXPOSURE TIME, PERCENT RETINAL BURNS, AND AVERAGE BURN SIZE, SHOT ORANGE

Station	Number of Rabbits	Condition of Eye	Retinal Burns	Average Lesion Diameter
			pct	mm
USS Boxer	8	Open	0	—
USS Epperson	8	Open	100	0.8
USS DeHaven	8	Open	—	—
C-97	8	Open	87.5	0.4

TABLE 3.5 COMPARISON OF ESTIMATED AND MEASURED RADIANT EXPOSURES, IMAGE AND LESION DIAMETERS

Station	Slant Range from Burst Point	Estimated Radiant Exposure at Observation Point	Measured Radiant Exposure at Observation Point	Estimated Fireball Image Diameter *	Measured Retinal Lesion Diameter
	naut mi	cal/cm²	cal/cm²	mm	mm
Shot Teak:					
Johnston Island	41	1.17	1.2	0.98	2.2
USS DeHaven	79	0.23	0.27	0.63	1.6
USS Cogswell	155	0.05	0.006	0.35	0.99
USS Hitchiti	307	0.005	0.0007 †	0.19	—
B-36 No. 1	73.8	0.36	—	0.76	1.8
B-36 No. 2	73.8	0.36	—	0.76	1.8
C-97	307	0.015 ‡	0.015	0.19	0.5
Shot Orange:					
USS Boxer	73	0.25	0.07 †	0.42	—
USS Epperson	88	0.15	0.075	0.36	0.8
USS DeHaven	141	0.085	0.007 †	0.23	—
C-97	336	0.028 ‡	0.0035	0.14	0.4

* Based on predicted fireball diameters used in the calculations in Chapter 1.

† Scattered thermal radiation.

‡ Assumes 50-percent transmission through plexiglass aircraft windows.

shot. Table 3.3 also shows the type of cloud cover at shot time for the various exposure stations and whether the line of sight to the detonation point was obstructed, as well as the diameter of representative lesions. Figure 3.2 is a photograph of the cloud cover at shot time at the 141-mile ground station. Table 3.4 indicates the condition of the rabbits' eyes at time of detonation, the percent of retinal burns, and average size of the burns.

3.3 SUMMARY

A summary of the comparisons between the preshot estimates and postshot measurements of physical parameters is contained in Table 3.5.

Chapter 4
DISCUSSION

There are two major problems facing the flier who is exposed to a nuclear detonation—flashblindness and chorioretinal burns. Flashblindness is a term used to designate a transient loss of vision following the exposure of the retinal rods and cones to extremely bright light. It is a physiological response, results from the depletion of the photosensitive chemical substances within the rod and cone cells, and varies in time (from 1 second to several minutes) according to the duration and intensity of the light exposure. There is no anatomic change produced, and the vision returns to its previous level of acuity.

The second category of primary disturbance is that of chorioretinal burns, an actual destruction of the percipient cells of the retina. Here again, the severity of the anatomical lesion and the final integrity of visual ability are dependent upon the magnitude and duration of exposure. The burns can be caused by energy released in the infrared or in the visible light spectra. The actual mechanism of production of the burns is simple; if intense light falls upon the retina at a fast rate of application so that heat is absorbed into the cellular elements faster than it can be dissipated by the chorioidal circulation, then heat accumulates within the cells and a burn results. The actual absorption of heat occurs in the pigment epithelium of the retina. If there is a slight excess above tolerance, only the pigment epithelium may be damaged; a somewhat greater excess will damage the rod and cone cells, resulting clinically in a scotoma (a non-seeing area in the visual field corresponding to the anatomic area of destruction of retinal cells). A still greater excess of heat may destroy not only these elements but also the overlying nerve-fiber layer which carries impulses from the peripheral retina; clinically, this would result in a wedge-shaped sector defect in the visual field with its apex at the burn site.

The degree of incapacity following a chorioretinal burn will also be dependent upon the severity of the lesion. Simultaneously with the production of the burn, there appears in the undestroyed tissue a halo of edema, which again is variable in extent. At some time following the injury, the inflammatory process spreads into the vitreous body, causing haziness and perhaps the appearance of floaters. Once again, these features are quite variable. Finally, the inflammatory response of the globe as a whole—sclera, chorioid, ciliary body, and other portions—is determined by the extent of the destructive lesion. With so many factors to be considered, therefore, the incapacity which follows a chorioretinal burn cannot be predicted with any accuracy. By its very nature of visual impairment, however, any amount of such handicap is critical to one who flies aircraft.

4.1 TECHNIQUE

The fundus lesions were measured as follows: the comparative unit of measure was arbitrarily determined to be 1 grid square, using the grid aperture of the standard Welsh-Allyn direct ophthalmoscope (May-type head). The diameter of the lesion was recorded as x-number of grid squares. The diameter of the chorioretinal lesion of one animal was measured in grid squares before death; after death, the animal's eye was opened and the lesion actually measured with a fine caliper. The actual size of the retinal lesion was 2 mm in diameter as measured with the calipers and 5 grid squares in diameter as measured with the ophthalmoscope. Therefore 1 grid was equal to 0.4 mm. The size of all chorioretinal lesions was calculated using 0.4 mm per grid.

41-mile surface station.

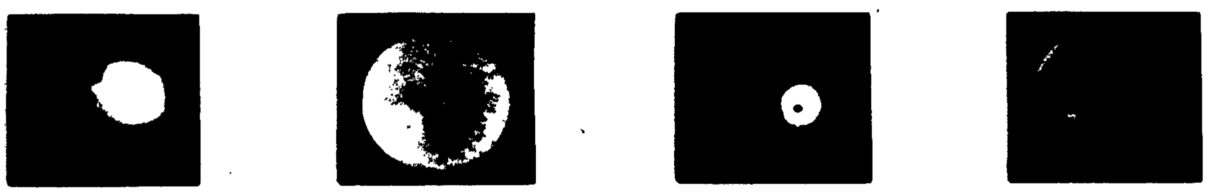

79-mile surface station.

155-mile surface station.

73.8-mile air station (B-36 No. 1).

Figure 4.1 Retinal burns in rabbit eyes at four stations, Shot Teak.

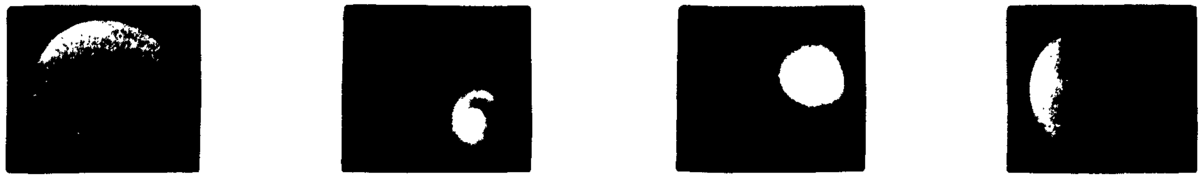

73.8-mile air station (B-36 No. 2), Shot Teak.

307-mile air station, Shot Teak.

226-mile air station, Shot Orange.

88-mile surface station, Shot Orange.

Figure 4.2 Retinal burns in rabbit eyes at four stations, Shots Teak and Orange.

Figure 4.3 Retinal lesion in left eye of Rabbit 70 exposed to Shot Teak at 41-mile surface station and photographed at H+10 hours. White oval lesion with a yellowish-red halo surrounds a granular blackish-yellow area in the center. It has 3 diopters of elevation and is approximately 2.40 mm in diameter. Subsequent examinations revealed that the lesion became a mottled black-and-white area without elevation. However, the lesion subtended the same diameter as initially.

Figure 4.4 Retinal lesion in right eye of Rabbit 35 exposed to Shot Teak at 73.8-mile air station (B-36 No. 2) and photographed at H + 26 hours. White circular lesion with red hemorrhage is surrounded by a grayish-white area in the center. Gray area is surrounded concentrically by a white halo, gray area, and finally a yellow linear area. Lesion is elevated 3 diopters and is 2.0 mm in diameter.

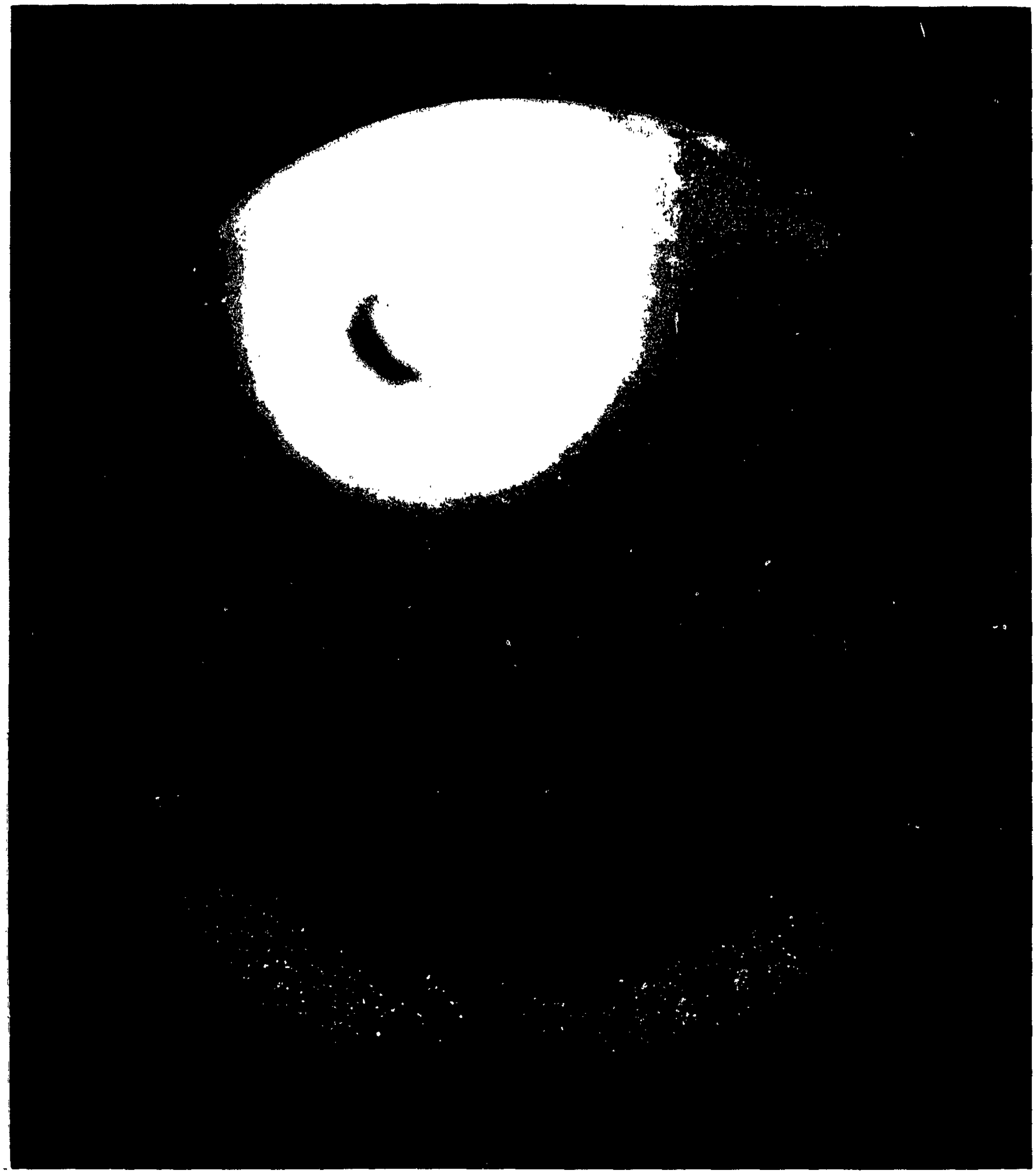

Figure 4.5 Retinal lesion in left eye of Rabbit 33 exposed to Shot Teak at 73.8-mile air station (B-36 No. 1) and photographed at H + 26 hours. Circular fluffy white lesion with a hole is surrounded by red pigment in its center. It is elevated 4 diopters and is 180 mm in diameter.

Figure 4.6 Retinal lesion in left eye of Rabbit 56 exposed to Shot Teak at 79-mile surface station and photographed at H + 12 hours. Circular white lesion with a gray star-shape is surrounded by white. Superiorly, there is red pigment; inferiorly, a floral-shaped area. This is surrounded by concentric rings from within—outward of yellow, red, and yellow colors. The lesion has 3 diopters of elevation and is 2.0 mm in diameter. Subsequent examinations showed lesion as wide as when first examined, but the elevation (edema) was gone and it was black and white in color.

Figure 4.7 Retinal lesion in left eye of Rabbit 75 exposed to Shot Teak at 155-mile surface station and photographed at H + 11 hours. It is a pearly white oval-shaped lesion with a reddish center and has a peripheral yellowish halo. It has 1 diopter of elevation and is 0.91 mm in diameter.

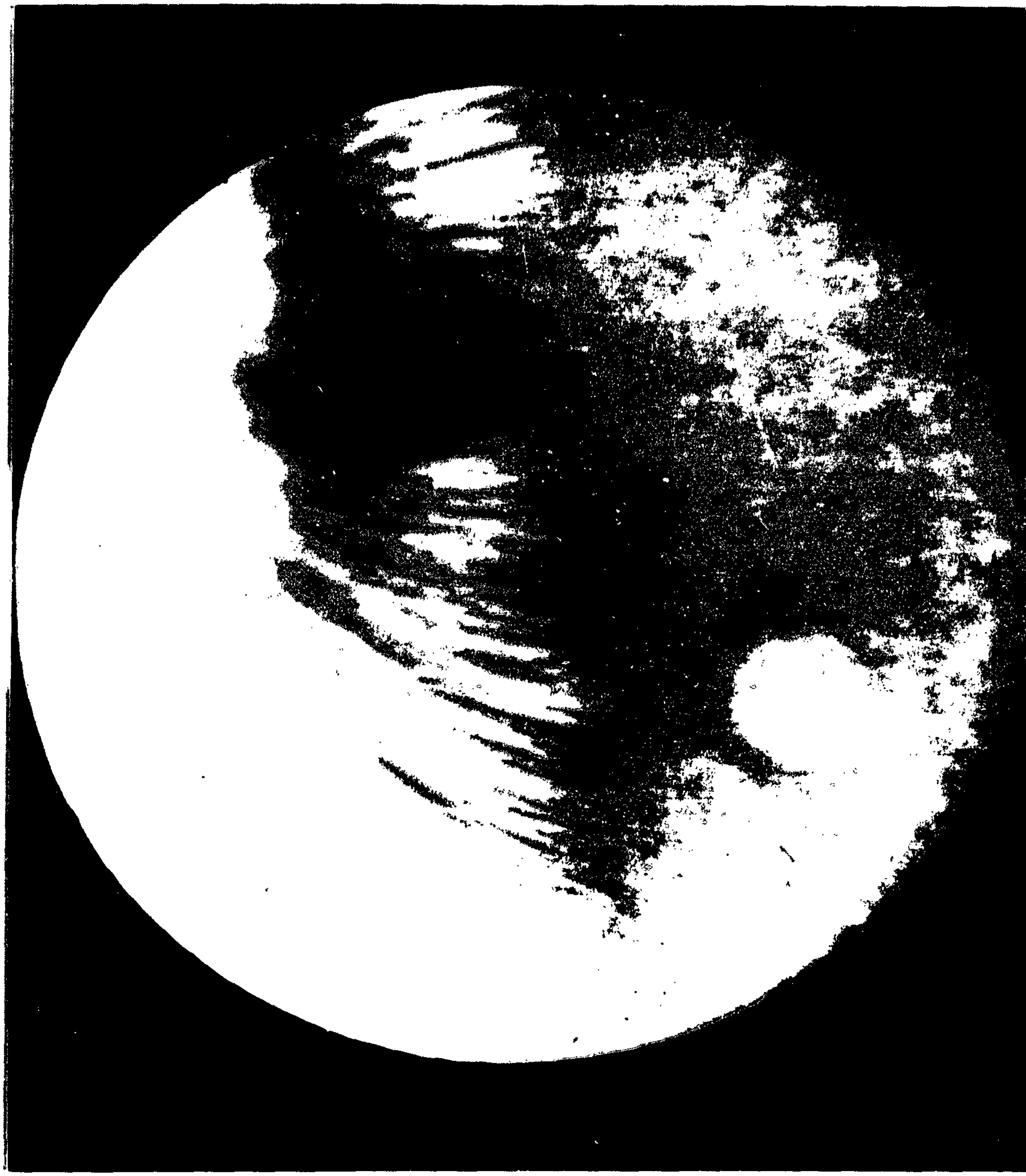

Figure 4.8 Retinal lesion in right eye of Rabbit 43 exposed to Shot Teak at 307-mile air station and photographed at H + 26 hours. It is a circular lesion with a white center surrounded concentrically by a black ring and a yellow peripheral area. It has questionable edema and is 0.53 mm in diameter. Subsequently, the lesion became much smaller.

Figure 4.9 Photomicrograph of retinal lesion in left eye of Rabbit 70 exposed to Shot Teak at 41-mile surface station. Histology: This section shows an area of retina with a loss of its pigment epithelium, rod and cone layer, and outer nuclear layer. The inner nuclear layer is disorganized, and the inner molecular layer is cystic and disorganized. Adjacent to this area, there are scattered clumps of retinal pigment and disorganized retina.

Figure 4.10 Photomicrograph of retinal lesion in right eye of Rabbit 35 exposed to Shot Teak at 73.8-mile air station (B-36 No. 2). Histology: An area not shown in this photograph had totally lost the retinal layers. Except for the pigment in the chorioid, all pigment has been dispersed from the area. Large areas adjacent to the severely scarred area have disrupted retina and chorioid. Glial tissue is present in the vitreous cavity of the globe.

Figure 4.11 Photomicrograph of retinal lesion in left eye of Rabbit 33 exposed to Shot Teak at 73.8-mile air station (B-36 No. 1). Histology: Magnification approximately 600 times. Whole area of lesion not shown. In the original slide, just to the right of the retinal fold (artefact), the pigment epithelium is present in clumps only. In the section shown in the photograph, the pigment epithelium is disrupted and the remainder of the retina completely disorganized. Apparently, much of the tissue pictured, especially in the area to the right of the lesion, is glial tissue.

Figure 4.12 Photomicrograph of retinal lesion in left eye of Rabbit 56 exposed to Shot Teak at 79-mile surface station. Histology: This section shows an area of disorganized chorioid, loss of pigment epithelium, loss of rods and cones, and dissolution of the remaining retinal layers.

Figure 4.13 Photomicrograph of retinal lesion in left eye of Rabbit 75 exposed to Shot Teak at 155-mile surface station. Histology: This section demonstrates an area with clumping of the pigment epithelium, loss of rods and cones, and disorganization of the outer retinal layers. The inner nerve-fiber layer has an increase in macrophages.

4.2 CLINICAL FINDINGS

All the animals had their eyes open at the time of the burst. Each exposed eye received a retinal burn (determined ophthalmoscopically) except those at the 305-mile surface station where no retinal injury was clinically visible. The size of the retinal lesions varied inversely with the slant-range distance from the burst. For Shot Teak, the average diameters were as follows: 41-mile surface station, 2.2 mm; 73.8-mile air stations, 1.8 mm; 79-mile surface station, 1.6 mm; 155-mile surface station, 0.99 mm; and the 307-mile air station, 0.5 mm.

The clinical appearance of the retinal lesions varied both in size and severity according to the distance from the burst. At the 41-mile surface station, 74-mile air stations, and 79-mile surface station, the burns showed either a central area of hemorrhage or a bright yellowish-white region of bared sclera (several burns showed both); this central region was surrounded by concentric rings of edema, which decreased in magnitude toward the periphery of the lesion. The burns at the 155-mile surface station were severe but did not show hemorrhage or the deeply penetrating hole; they did have the concentric rings of edema, decreasing peripherally. At the 307-mile air station, the lesions were minimal by comparison and consisted almost entirely of superficial edema; permanent scarring was dependent upon size.

Figures 4.1 and 4.2 show four retinal burns from each station at which burns were received during Shots Teak and Orange. Figures 4.3 through 4.8 are enlarged photographs of representative burns from each station during Shot Teak and a clinical description of each.

The burns received during Shot Orange were comparable clinically to those from Shot Teak and are not shown enlarged or described.

4.3 HISTOLOGY

The severity of the retinal damage from Shot Teak may be estimated from the histologic photomicrographs made several months after exposure. These photomicrographs, Figures 4.9 through 4.13, are the same eyes shown in Figures 4.3 through 4.7. The histologic description is given with each figure. The lesions caused by Shot Orange were comparable histologically to those of Shot Teak and are not shown or described.

4.4 SIGNIFICANCE OF LESIONS

The largest lesions occurred at the nearest station and extended from the mid-periphery to the outer extremity of the retina. At 79 miles, the burns were smaller and located in the mid-periphery; at 155 miles, the burns were still smaller and very near the posterior pole. The rabbits in the 73.8-mile air stations developed lesions which were quite large (only slightly smaller than at the nearest station) but not so peripherally located. At the 307-mile air station, all lesions were small and located at or very near the macula.

In all of the eyes in which retinal burns were produced, the immediate problem of flashblindness would produce an incapacitating visual loss of significant degree. In addition, the large lesions would cause an instantaneous inflammatory reaction lasting many weeks and certainly leaving some permanent loss of visual acuity because of a hazy media. The intermediate-sized lesions would also produce an intra-ocular inflammation, its severity and duration depending upon the size of the burn. In the eyes with the smallest burns, the flashblindness would be the chief concern unless the burn was in the macular area.

Permanent visual defects would depend upon the size and location of the final scar. The large peripheral scars would probably produce a peripheral visual field defect corresponding to the location of the scar. The intermediate lesions would result in a sector field defect with its apex at the site of the lesion. The smallest burns would produce scotomatous field defects; in this case, the eventual effect on central vision depends upon proximity of the scar to the fovea—final central vision might be as low as 20/70 or less.

[illegible]

[illegible]

[illegible]

[illegible]

[illegible]

[illegible] and/or [illegible]

[illegible]

[illegible]

[illegible] of the [illegible] as in the case of [illegible] in the present case [illegible]

[illegible]

[illegible]

[redacted]

[redacted]

[redacted]

[redacted]

[redacted]

REFERENCES

1. V. A. Byrnes and others: "Ocular Effects of Thermal Radiation from Atomic Detonation—Flashblindness and Chorioretinal Burns"; Project 4.5, Operation Upshot-Knothole, WT-745, November 1955; School of Aviation Medicine, USAF, Randolph Field, Texas; Unclassified.

2. R. S. Fixott and others: "Chorioretinal Burns"; Project 4.1, Operation Redwing, WT-[illegible], March [illegible]; School of Aviation Medicine, USAF, Randolph Air Force Base, Texas; Secret Formerly Restricted Data.

3. W. E. Gibbons and others: "Evaluation of Eye Protection Afforded by an Electromechanical Shutter"; Project 4.2, Operation Plumbbob, WT-[illegible], April [illegible]; Aero Medical Laboratory, Wright Air Development Center, Wright-Patterson Air Force Base, Ohio; Unclassified.

4. William Ogle: Personal Communication. Subject: "Operation Hardtack," May 1958; Secret Restricted Data.

5. W. T. Ham, Jr.: "Flash Burns in the Rabbit Retina"; Scientific Progress Report, Contract AF 18([illegible]), April [illegible]; School of Aviation Medicine, USAF, Randolph Air Force Base, Texas; Unclassified.

6. Thomas Shipman: Personal Communication. Subject: "Operation Hardtack," May 1958; Unclassified.

7. Herman Hoerlin: Personal Communication. Subject: "Operation Hardtack," August 1958; Secret Restricted Data.

SECRET

Appendix

MEASUREMENT of INCIDENT THERMAL RADIATION

The thermal radiation was measured at each station at which [illegible] were exposed.

A.1 INSTRUMENTS

Two general types of instruments — calorimeters and photocells — were used at each station. The calorimeters measured the total amount of thermal radiant energy (summed over the duration of the shot) which fell on a unit area of an imaginary plane oriented to face the fireball. The photocells measured, only roughly, the rate at which the thermal radiant energy fell at each instant. The photocells were also to furnish some information on the spectral character of the radiation.

A.1.1 Calorimeters. The calorimeters were of a spectrally nonselective type. These included the familiar, blackened, copper-button calorimeter designed and constructed by the Naval Radiological Defense Laboratory (NRDL) and similar units constructed at the Naval Material Laboratory (NML). Some of the NML types were designed with special characteristics, such as extreme thinness, to provide high sensitivity and fast response. All types of these instruments had been used successfully in a number of previous nuclear tests by NML and others.

The NML calorimeters consisted of thin copper bodies, 0.0025 to 0.013 cm thick, and up to 1½ inches long. The exposed surface had been blackened with carbon black. The bodies were mounted in metal housings with thin quartz windows. The temperatures of the bodies were recorded continuously during and for seconds after each shot by means of thin-wire thermocouples soldered or pressed to the backs of the bodies. The outputs of the thermocouples were fed into a Heiland recording oscillograph equipped with Heiland [illegible] galvanometers. These galvanometers had a response that was flat within 5 percent from 0 to [illegible] cps.

For the calibration of the NML calorimeters, with thickness 0.01 cm or more, the sensitivity was calculated from the thickness and thermal capacity of the copper body, with correction for attenuation at the quartz window and the blackened receiving surface. The NRDL calorimeters and the thin NML calorimeters were calibrated in the laboratory by comparison with other instruments. The heat-loss rate was determined for each calorimeter from the temperature record made immediately after each shot.

The window of the housing was large enough to permit radiation to enter the copper body at all angles of incidence up to almost 90 degrees. For this reason, the readings of thermal radiant energy given by these instruments included not only energy received directly from the fireball but also energy scattered by the air and clouds.

A.1.2 Photocells. The photocells were silicon photovoltaic cells that were sensitive to radiation of wave length between 400 and 1,000 mμ, with peak sensitivity at 800 mμ. Neutral filters of aluminized glass and of exposed, developed photographic film were used. The output of most of the photocells was fed through a suitable electrical network into the same type of galvanometer used with the calorimeters; for a few photocells, Heiland 1000 D galvanometers, which had a frequency response flat to 600 cps, were used.

The linearity, relative sensitivity, and time-response characteristics of the photocells and their circuits were recorded for each circuit at each station, as finally connected. This was done by means of specially constructed calibrators, which consisted of a calibrated incandescent lamp behind a chopper wheel with circular apertures. Each aperture was covered with a different neutral filter of known transmittance.

A.2 STATION DESIGN

The intensity of radiation was not known beforehand to project personnel, and so a number of calorimeters of different sensitivity and a number of photocells with networks providing a range of sensitivity were used at each station. This increased the probability of obtaining at least one usable oscillograph trace for each type of instrument at each station.

The calorimeters and photocells at each station were mounted on one or two rigid metal panels and oriented so as to face the expected position of the fireball.

A.3 RESULTS

A.3.1 Calorimeter Readings. The results taken from the usable calorimeter traces are given in Table A.1. For the [illegible] and C-9T stations during [illegible], these are not to be taken as the best estimates of thermal intensity, as mentioned in Section A.3.6.

A.3.2 Photocell Readings. During Shot Teak, the photocell traces went off scale at the beginning of the shot, except for two or three cases, and then dropped back on scale in a smooth curve that in some cases showed one small pip. Table A.2 indicates the shape of this curve by giving normalized deflections for five values of elapsed time after time zero. The first value was chosen to be the first time during which a representative number of traces were back on scale.

During Shot Orange, the photocell traces rose in 0.005 second to a level which was maintained within a few percent for about 0.17 second, whereupon the trace dropped close to its zero line in another 0.05 second. An attempt to relate the amplitude of the deflection with the calorimeter reading at the same station, as was done by the normalization of Table A.2, showed greater discrepancies than can be explained as experimental error.

A.3.3 Angular Correction. During Shot Teak, the average roll of the USS DeHaven was 3.5 degrees and of the USS Cogswell, 5 degrees. At zero time for Shot Orange, the USS Epperson had rolled 2.5 degrees away from the fireball and the USS DeHaven, 1.3 degrees away; the amplitude of roll of the USS Boxer was negligible. The amount of pitch of all of the ships was negligible. The deviation from correct heading was in no case greater than 5 degrees. Inasmuch as the error caused by improper orientation of the calorimeters and photocells was an insensitive function of angle for small angles of error, no corrections on this account were made for the ship stations or the C-97 aircraft.

TABLE A.1 CALORIMETER READINGS

Station	Oscillograph Trace Number	Thermal Intensity (Radiant Exposure)
		cal/cm^2
Shot Teak:		
Johnston Island	1 and 5	1.2
	1 and 6	1.3
	1 and 11	1.0
	2 and 5	1.3
	Average	1.2
USS DeHaven	5	0.26
	6	0.31
	8	0.30
	9	0.22
	Average	0.27
USS Cogswell	5	0.053
	6	0.079
	Average	0.066
USS Hitchiti *	Deflection too small to measure	
C-97	4	0.0110 †
Shot Orange:		
USS Boxer *	3	0.07
	11	0.06
	12	0.09
	Average	0.07
USS Epperson	4	0.06
	6	0.09
	Average	0.075
USS DeHaven *	2	0.008
	5	0.006
	Average	0.007
C-97	4	0.0035

* Direct line of sight to fireball interrupted by clouds.

† See best estimate of thermal intensity in Table A.3.

No pitch, roll, or heading information were available for the USS Hitchiti. However, the direct line of sight for this ship was interrupted by clouds, and so any reasonable errors in orientation would not be significant.

TABLE A.2 PHOTOCELL READINGS, SHOT TEAK

Values are raw deflections divided by the product of the average calorimeter reading at the station (from Table A.1), the filter transmittance, and the sensitivity of the photocell.

Station	Oscillograph Trace Number	Normalized Deflection Interval After Zero Time: 20 msec	40 msec	60 msec	80 msec	100 msec
		Arbitrary Units				
Johnston Island	7	26	15	9	5.7	3.9
	8	23	13	8	4.9	3.2
USS DeHaven	2	25	14	9	6.2	4.3
USS Cogswell	3	25	15	9	6.1	4.3
	4	OS *	OS *	OS *	5.9	4.3
USS Hitchiti	1	25 †	15 †	10 †	6.7 †	4.8 †
C-97	1	54	31	20	14	10
	2	OS *	27	17	12	9

* Off scale.

† The values for the USS Hitchiti could not be normalized as the others were, because no calorimeter was available from Table A.1. Instead, to facilitate comparison of the curve with the others, the USS Hitchiti readings were simply normalized to make the 20-msec reading equal 25.

<u>A.3.4 Spectral Character of Radiation.</u> The fact that the data of Table A.2 show the same shape of curve for each station in Shot Teak indicates that, for the wave-length region in which the photocells were sensitive, either the relative spectral emittance of the fireball did not vary greatly with time or else the atmosphere was not significantly selective in its transmittance. For the Johnston Island, USS DeHaven, and USS Cogswell stations, the normalized values were almost identical for each station. This indicates that the ratio of the radiant energy incident at any fixed instant, in the wave-length region in which these cells were sensitive to the total incident radiant energy, was constant for these stations. The fact that the values for the C-97, which was at a much greater range than the above three stations, were double the others indicates that either the proportion of energy in the sensitive region of the photocells had increased with distance or else the calorimeter reading for the C-97 station was in error. The latter explanation seems more likely, because there is no evidence of spectral changes among the first three stations.

TABLE A.3 CORRECTED VALUES OF RADIANT EXPOSURE

Station	Radiant Exposure
	cal/cm^2
Shot Teak:	
Johnston Island	1.2
USS DeHaven	0.27
USS Cogswell	0.066
USS Hitchiti *	0.0007
C-97	0.015
Shot Orange:	
USS Boxer *	0.07
USS Epperson	0.075
USS DeHaven *	0.007
C-97	0.0035

* Direct line of sight to fireball interrupted by clouds.

During Shot Orange, the photocell traces again had nearly the same shape from station to station, leading to the same conclusion as was reached in the first sentence of the previous paragraph.

A.3.5 Time Characteristic of Radiation. As stated in Section A.3.2, the photocell traces for Shot Teak differed markedly from those for Shot Orange. Although the same cells, networks, galvanometers, and operating conditions were used for both shots, there was apparently a real difference in the time characteristic of the two shots. An accurate estimate of the time characteristic of the thermal radiation cannot be made from the present data, because the photocells used were selective in their spectral response, and the ratio of energy in the sensitive wave-length region of the photocells to the total energy was probably not constant from instant to instant for the duration of the shot. A further complication lies in the fact that the time constant of the galvanometers may have been too great for the rate of fluctuation of the thermal radiation.

A.3.6 Radiant Exposure. Table A.2 shows that the ratio of the photocell readings to the average calorimeter reading was constant within about 5 percent from station to station for Johnston Island, USS DeHaven, and USS Cogswell in Shot Teak. This indicates that the random error in the calorimeter readings was within about 5 percent for these stations.

For the C-97 station, the ratio was close to double that for the other stations, indicating, as mentioned in Section A.3.4, either a spectral effect or, more likely, an error in the single calorimeter reading available for the C-97. Weighing these two possibilities equally results in a revised estimate of the thermal intensity at the C-97 station: namely, the value 0.015 cal/cm^2, with a random error within about 33 percent, instead of the value 0.010 cal/cm^2 given in Table A.1.

For the station on the USS Hitchiti during Shot Teak, where no calorimeter reading was obtained because of the low thermal intensity, similar reasoning based on the photocell readings gives 0.0007 cal/cm^2 as the best estimate of thermal intensity.

No correction of the calorimeter data of Shot Orange, on the basis of photocell data, can be made.

The corrected values of radiant exposure for Shots Teak and Orange are given in Table A.3.

DISTRIBUTION

Military Distribution Categories 42 and 82

ARMY ACTIVITIES

1 Deputy Chief of Staff for Military Operations, D/A, Washington 25, D.C. ATTN: Dir. of SW&R
2 Chief of Research and Development, D/A, Washington 25, D.C. ATTN: Atomic Div.
3 Assistant Chief of Staff, Intelligence, D/A, Washington 25, D.C.
4- 5 Chief Chemical Officer, D/A, Washington 25, D.C.
6 Chief of Engineers, D/A, Washington 25, D.C. ATTN: ENGNB
7 Chief of Engineers, D/A, Washington 25, D.C. ATTN: ENGEB
8 Chief of Engineers, D/A, Washington 25, D.C. ATTN: ENGTB
9- 10 Office, Chief of Ordnance, D/A, Washington 25, D.C. ATTN: ORDTN
11 Chief Signal Officer, D/A, Research and Development Div., Washington 25, D.C. ATTN: SIGRD-4
12 The Surgeon General, D/A, Washington 25, D.C. ATTN: MEDNE
13- 15 Commanding General, U.S. Continental Army Command, Ft. Monroe, Va.
16 Director of Special Weapons Development Office, Headquarters CONARC, Ft. Bliss, Tex. ATTN: Capt. Chester I. Peterson
17 President, U.S. Army Artillery Board, Ft. Sill, Okla.
18 President, U.S. Army Infantry Board, Ft. Benning, Ga.
19 President, U.S. Army Air Defense Board, Ft. Bliss, Tex.
20 President, U.S. Army Aviation Board, Ft. Rucker, Ala. ATTN: ATBG-DG
21 Commandant, U.S. Army Command & General Staff College, Ft. Leavenworth, Kansas. ATTN: ARCHIVES
22 Commandant, U.S. Army Air Defense School, Ft. Bliss, Tex. ATTN: Command & Staff Dept.
23 Commandant, U.S. Army Armored School, Ft. Knox, Ky.
24 Commandant, U.S. Army Artillery and Missile School, Ft. Sill, Okla. ATTN: Combat Development Department
25 Commandant, U.S. Army Aviation School, Ft. Rucker, Ala.
26 Commandant, U.S. Army Infantry School, Ft. Benning, Ga. ATTN: C.D.S.
27 The Superintendent, U.S. Military Academy, West Point, N.Y. ATTN: Prof. of Ordnance
28 Commandant, The Quartermaster School, U.S. Army, Ft. Lee, Va. ATTN: Chief, QM Library
29 Commandant, U.S. Army Ordnance School, Aberdeen Proving Ground, Md.
30 Commandant, U.S. Army Ordnance and Guided Missile School, Redstone Arsenal, Ala.
31 Commanding General, Chemical Corps Training Comd., Ft. McClellan, Ala.
32 Commandant, USA Signal School, Ft. Monmouth, N.J.
33 Commandant, USA Transport School, Ft. Eustis, Va. ATTN: Security and Info. Off.
34 Commanding General, The Engineer Center, Ft. Belvoir, Va. ATTN: Asst. Cmdt, Engr. School
35 Commanding General, Army Medical Service School, Brooke Army Medical Center, Ft. Sam Houston, Tex.
36 Director, Armed Forces Institute of Pathology, Walter Reed Army Med. Center, 625 16th St., NW, Washington 25, D.C.
37 Commanding Officer, Army Medical Research Lab., Ft. Knox, Ky.
38 Commandant, Walter Reed Army Inst. of Res., Walter Reed Army Medical Center, Washington 25, D.C.
39- 41 Commanding General, QM R&D Comd., QM R&D Cntr., Natick, Mass. ATTN: CBR Liaison Officer
42 Commanding General, Qm. Research and Engr. Comd., USA, Natick, Mass.
43- 44 Commanding General, U.S. Army Chemical Corps, Research and Development Comd., Washington 25, D.C.
45- 46 Commanding Officer, Chemical Warfare Lab., Army Chemical Center, Md. ATTN: Tech. Library
47 Commanding General, Engineer Research and Dev. Lab., Ft. Belvoir, Va. ATTN: Chief, Tech. Support Branch
48 Director, Waterways Experiment Station, P.O. Box 631, Vicksburg, Miss. ATTN: Library
49 Commanding Officer, Diamond Ord. Fuze Labs., Washington 25, D.C. ATTN: Chief, Nuclear Vulnerability Br. (230)
50- 51 Commanding General, Aberdeen Proving Grounds, Md. ATTN: Director, Ballistics Research Laboratory
52 Commander, Army Ballistic Missile Agency, Redstone Arsenal, Ala. ATTN: ORDAB-HT
53 Commanding General, U.S. Army Electronic Proving Ground, Ft. Huachuca, Ariz. ATTN: Tech. Library
54 Commanding Officer, USA, Signal R&D Laboratory, Ft. Monmouth, N.J. ATTN: Tech. Doc. Ctr., Evans Area
55 Director, Operations Research Office, Johns Hopkins University, 6935 Arlington Rd., Bethesda 14, Md.
56 Commandant, U.S. Army Chemical Corps, CBR Weapons School, Dugway Proving Ground, Dugway, Utah.
57 Commander-in-Chief, U.S. Army Europe, APO 403, New York, N.Y. ATTN: Opot. Div., Weapons Br.
58 Commanding General, Southern European Task Force, APO 168, New York, N.Y. ATTN: ACofS G-3
59 Commanding Officer, 9th Hospital Center, APO 180, New York, N.Y. ATTN: CO, US Army Nuclear Medicine Research Detachment, Europe

NAVY ACTIVITIES

60- 61 Chief of Naval Operations, D/N, Washington 25, D.C. ATTN: OP-03EG
62 Chief of Naval Operations, D/N, Washington 25, D.C. ATTN: OP-75
63 Chief of Naval Operations, D/N, Washington 25, D.C. ATTN: OP-91
64 Chief of Naval Operations, D/N, Washington 25, D.C. ATTN: OP-922G2
65 Chief of Naval Personnel, D/N, Washington 25, D.C.
66- 67 Chief of Naval Research, D/N, Washington 25, D.C. ATTN: Code 811
68- 70 Chief, Bureau of Naval Weapons, D/N, Washington 25, D.C. ATTN: DLI-3
71- 75 Chief, Bureau of Naval Weapons, D/N, Washington 25, D.C. ATTN: RAAD-25
76 Chief, Bureau of Medicine and Surgery, D/N, Washington 25, D.C. ATTN: Special Wpns. Def. Div.
77 Chief, Bureau of Ordnance, D/N, Washington 25, D.C.
78 Chief, Bureau of Naval Weapons, D/N, Washington 25, D.C. ATTN: SP-43
79 Chief, Bureau of Ships, D/N, Washington 25, D.C. ATTN: Code 423
80 Chief, Bureau of Yards and Docks, D/N, Washington 25, D.C. ATTN: D-440
81 Director, U.S. Naval Research Laboratory, Washington 25, D.C. ATTN: Mrs. Katherine H. Cass
82- 83 Commander, U.S. Naval Ordnance Laboratory, White Oak, Silver Spring 19, Md.
84- 85 Director, Material Lab. (Code 900), New York Naval Shipyard, Brooklyn 1, N.Y.
86 Commanding Officer and Director, Navy Electronics Laboratory, San Diego 52, Calif.
87 Commanding Officer, U.S. Naval Mine Defense Lab., Panama City, Fla.
88- 91 Commanding Officer, U.S. Naval Radiological Defense Laboratory, San Francisco, Calif. ATTN: Tech. Info. Div.
92 Commanding Officer and Director, U.S. Naval Civil Engineering Laboratory, Port Hueneme, Calif. ATTN: Code L31

93 Commanding Officer, U.S. Naval Schools Command, U.S. Naval Station, Treasure Island, San Francisco, Calif.

94 Superintendent, U.S. Naval Postgraduate School, Monterey, Calif.

95 Officer-in-Charge, U.S. Naval School, CEC Officers, U.S. Naval Construction Bn. Center, Port Hueneme, Calif.

96 Commanding Officer, Nuclear Weapons Training Center, Atlantic, U.S. Naval Base, Norfolk 11, Va. ATTN: Nuclear Warfare Dept.

97 Commanding Officer, Nuclear Weapons Training Center, Pacific, Naval Station, San Diego, Calif.

98 Commanding Officer, U.S. Naval Damage Control Tng. Center, Naval Base, Philadelphia 12, Pa. ATTN: ABC Defense Course

99 Commanding Officer, Air Development Squadron 5, VX-5, China Lake, Calif.

100 Commanding Officer, Naval Air Material Center, Philadelphia 12, Pa. ATTN: Technical Data Br.

101 Commanding Officer, U.S. Naval Air Development Center, Johnsville, Pa. ATTN: NAS, Librarian

102 Officer-in-Charge, U.S. Naval Supply Research and Development Facility, Naval Supply Center, Bayonne, N.J.

103 Commandant, U.S. Marine Corps, Washington 25, D.C. ATTN: Code AO3H

104 Director, Marine Corps Landing Force, Development Center, MCS, Quantico, Va.

105 Commanding Officer, U.S. Naval CIC School, U.S. Naval Air Station, Glynco, Brunswick, Ga.

106 Chief of Naval Operations, Department of the Navy, Washington 25, D.C. ATTN: OP-09B5

107-115 Chief, Bureau of Naval Weapons, Navy Department, Washington 25, D.C. ATTN: RR12

AIR FORCE ACTIVITIES

116 Hq. USAF, ATTN: Operations Analysis Office, Office, Vice Chief of Staff, Washington 25, D. C.

117 Director of Civil Engineering, HQ. USAF, Washington 25, ATTN: AFOCE

118-128 Air Force Intelligence Center, HQ. USAF, ACS/I (AFCIN-3V1) Washington 25, D.C.

129 Director of Research and Development, DCS/D, HQ. USAF, Washington 25, D.C. ATTN: Guidance and Weapons Div.

130 The Surgeon General, HQ. USAF, Washington 25, D.C. ATTN: Bio.-Def. Pre. Med. Division

131 Commander, Tactical Air Command, Langley AFB, Va. ATTN: Doc. Security Branch

132 Commander, Air Defense Command, Ent AFB, Colorado. ATTN: Assistant for Atomic Energy, ADLDC-A

133 Commander, Hq. Air Research and Development Command, Andrews AFB, Washington 25, D.C. ATTN: RDRWA

134 Commander, Air Force Ballistic Missile Div. HQ. ARDC, Air Force Unit Post Office, Los Angeles 45, Calif. ATTN: WDSO

135-136 Commander, AF Cambridge Research Center, L. G. Hanscom Field, Bedford, Mass. ATTN: CRQST-2

137-141 Commander, Air Force Special Weapons Center, Kirtland AFB, Albuquerque, N. Mex. ATTN: Tech. Info. & Intel. Div.

142-143 Director, Air University Library, Maxwell AFB, Ala.

144 Commander, Lowry Technical Training Center (TW), Lowry AFB, Denver, Colorado.

145-146 Commandant, School of Aviation Medicine, USAF, Aerospace Medical Center (ATC), Brooks Air Force Base, Tex. ATTN: Col. Gerritt L. Hekhuis

147 Commander, 1009th Sp. Wpns. Squadron, HQ. USAF, Washington 25, D.C.

148-149 Commander, Wright Air Development Center, Wright-Patterson AFB, Dayton, Ohio. ATTN: WCACT (For WCOSI)

150-151 Director, USAF Project RAND, VIA: USAF Liaison Office, The RAND Corp., 1700 Main St., Santa Monica, Calif.

152 Commander, Air Defense Systems Integration Div., L. G. Hanscom Field, Bedford, Mass. ATTN: SIDE-S

153 Commander, Air Technical Intelligence Center, USAF, Wright-Patterson AFB, Ohio. ATTN: AFCIN-4B1a, Library

154 Assistant Chief of Staff, Intelligence, HQ. USAFE, APO 633, New York, N.Y. ATTN: Directorate of Air Targets

155 Commander-in-Chief, Pacific Air Forces, APO 953, San Francisco, Calif. ATTN: PFCIE-MB, Base Recovery

OTHER DEPARTMENT OF DEFENSE ACTIVITIES

156 Director of Defense Research and Engineering, Washington 25, D.C. ATTN: Tech. Library

157 Director, Weapons Systems Evaluation Group, Room 1E880, The Pentagon, Washington 25, D.C.

158-161 Chief, Defense Atomic Support Agency, Washington 25, D.C. ATTN: Document Library

162 Commander, Field Command, DASA, Sandia Base, Albuquerque, N. Mex.

163 Commander, Field Command, DASA, Sandia Base, Albuquerque, N. Mex. ATTN: FCTG

164-165 Commander, Field Command, DASA, Sandia Base, Albuquerque, N. Mex. ATTN: FCWT

166 Commander, JTF-7, Arlington Hall Station, Arlington 12, Va.

167 Administrator, National Aeronautics and Space Administration, 1520 "H" St., N.W., Washington 25, D.C. ATTN: Mr. R. V. Rhode

168 Commander-in-Chief, Strategic Air Command, Offutt AFB, Neb. ATTN: OAWS

169 Commandant, US Coast Guard, 1300 E. St., N.W., Washington 25, D.C. ATTN: (OIN)

170 U.S. Documents Officer, Office of the United States National Military Representative - SHAPE, APO 55, New York, N.Y.

ATOMIC ENERGY COMMISSION ACTIVITIES

171-173 U.S. Atomic Energy Commission, Technical Library, Washington 25, D.C. ATTN: For DMA

174-175 Los Alamos Scientific Laboratory, Report Library, P.O. Box 1663, Los Alamos, N. Mex. ATTN: Helen Redman

176-180 Sandia Corporation, Classified Document Division, Sandia Base, Albuquerque, N. Mex. ATTN: H. J. Smyth, Jr.

181-190 University of California Lawrence Radiation Laboratory, P.O. Box 808, Livermore, Calif. ATTN: Clovis G. Craig

191 Weapon Data Section, Office of Technical Information Extension, Oak Ridge, Tenn.

192-225 Office of Technical Information Extension, Oak Ridge, Tenn. (Surplus)